Article

Comparison of the Performance of Hybrid Traffic Signal Patterns and Conventional Alternatives When Accounting for Both Pedestrians and Vehicles

Farzaneh Montazeri [1,*]**, Fausto Errico** [1] **and Luc Pellecuer** [2]

1   CIRRELT, GERAD and École de Technologie SupéRieure, 1100, Rue Notre-Dame Ouest,
     Montréal, QC H3C 1K3, Canada
2   School of Engineering, Faculty of Environment & Technology, University of the West of
     England (UWE Bristol), Frenchay Campus, Coldharbour Lane, Bristol BS16 1QY, UK
*   Correspondence: farzane.montazeri@gmail.com

Abstract: Traffic control systems are crucial for managing traffic flows. Their main function is to reduce interactions among users for safety reasons, while minimizing the travel times. Researchers often concentrate on the cycle length, whose impact on travel times is directly measurable. However, the choice of the signal pattern may also have a great potential to reduce travel times and unsafe situations. This potential is yet to be thoroughly investigated. In this work, we are interested in comparing different signal patterns in terms of the number of potential conflicts and delay time for both drivers and pedestrians. To this end, we first select three commonly adopted signal patterns, namely the Exclusive Pedestrian Phase (EPP), the Leading Through Interval (LTI) and the Two-Way Crossing (TWC). We then generalize existing methods for measuring user delay and safety for these three signal patterns. Moreover, we investigate a hypothetical hybrid pattern obtained by dynamically adapting the signal pattern to real-time data. The proposed methodology is applied to a case study considering an isolated intersection in Montreal, Canada. We perform computational experiments geared towards determining the best pattern according to ad hoc performance indicators and user flows. Results show that the EPP and LTI patterns generally perform better than TWC. EPP generally outperforms LTI when measuring the number of potential conflicts, while LTI outperforms EPP when considering delay times. Furthermore, the hypothetical hybrid pattern shows a positive but overall limited impact regarding both delay times and number of potential conflicts.

Keywords: traffic control; traffic signal optimization; pedestrians; safety; delay time; signal patterns; hybrid signal pattern

1. Introduction

With the increasing use of vehicles globally, transportation management and control systems have been developed to facilitate access by motorized users to roads and infrastructures and consequently increase the quality of the travel experience. The urban transportation system includes three general components: the infrastructure (roads, intersections, and bridges), users (vehicles, pedestrians, bicycles and drivers), and operation tools (signs, traffic signals and management and control systems). As a tool for traffic management in urban areas, the traffic signals feature different control approaches in terms of methods, technologies (hardware and software), and objectives. The common objectives of the traffic signal are to maximize vehicle throughput and intersection safety while minimizing travel time.

This paper focuses on how traffic signal control techniques may be adapted to consider pedestrian-related performance indicators to improve safety and travel time for an intersection. The control of traffic signals is a complex process since it involves many interrelated elements, such as safety, capacity, delay time, queue length, intersection geometries, heterogeneous users, and environmental conditions. All these elements affect the cycle length

(the time a traffic signal requires to complete the sequence of signal phases) and signal pattern (the set of user movements allowed at each phase of the signal cycle). The cycle length and the signal pattern represent essential elements in traffic signal investigation. Most traffic agencies nowadays are interested in the concept of an adaptive control system that applies real-time traffic data to change the cycle length and the pattern of a traffic signal dynamically [1].

In the literature, traffic signal control optimization is mainly geared towards minimizing the cycle length and improving measures that are directly or indirectly influenced by the cycle length. These measure include traffic capacity, travel time, system throughput, vehicle-to-vehicle conflict, and vehicle emissions [2–7]. All these measures mainly quantify vehicle-related performance. Pedestrian-related performance indicators have also been studied in the literature [4,8,9], but in most related works, interactions between pedestrians and vehicles were not explicitly considered.

In real-world intersections, traffic signal control may feature rather complex configurations of signal patterns. The literature, however, mostly focuses only on simple forms of traffic signal phase sequences and patterns (such as a two-phase traffic signal). Even works that focus on optimal cycle length models applied to different signal patterns [7,9,10], assume simplified intersection conditions with fixed traffic flow or one-way streets [10,11]. Similarly, one specific signal pattern is typically applied for the whole day whereas traffic flows largely change during the day, with a potential increase of delay time and travel time at the intersection [10]. Furthermore, since collecting pedestrian data has traditionally been costly and time-consuming, even advanced traffic control systems capable of dynamically adapting the cycle length to real-time data have not considered pedestrian users [1]. However, recent development in information technology allow to more easily collect and process real-time traffic data, thus enabling more complex signal control policies see [12], for example.

The most common signal patterns that explicitly consider interactions between motorized and non-motorized users are: Two-Way Crossing (TWC), Exclusive Pedestrian Phase (EPP), Leading Pedestrian Interval (LPI), and Leading Through Interval (LTI). In the literature, a trade-off between safety and delay time has been considered to measure the efficiency of each signal pattern [11]. Generally, to investigate the safety of intersections, the literature considers the number of accidents or predicted crash data [13–17]. Moreover, to estimate the intersection delay, several researchers have used the HCM delay model. However, their delay and safety models have usually failed to consider the effect of signal patterns or pedestrian data.

This paper aims to investigate whether continuously changing the pattern configuration throughout the day to adapt to real-time traffic flow fluctuations could improve the level of service at an intersection. This paper hypothesizes that considering both the delay time and the number of conflict situations in the design of such a hybrid pattern will decrease travel time and increase safety. This research is articulated around the following three objectives:

- To specify the methods for measuring real-time delay and number of conflict situations for relevant signal patterns (TWC, EPP, and LTI).
- To develop a case study to assess the impact of the different traffic signal patterns on delay time and safety using real-time traffic data.
- To investigate the effectiveness of dynamically changing signal patterns in improving traffic signal performance (i.e., decreased travel time and increased safety) while identifying the best performing pattern for each individual period of the case study.

The rest of the paper is organized as follows. Section 2 reviews the literature to identify the relevant signal patterns and performance indicator models. Section 3 details the methodological approach used in this study. Section 4 develops pedestrian-sensitive performance indicators and generates the delay time and potential conflict models for each signal pattern of the study. In Section 5, the results and limitation are discussed as the experimental setting is applied to a case study for a specific intersection in Montreal, using

real-time traffic data and Synchro software in the simulation phase to verify the impact of the hybrid signal pattern on the level of service at the intersection. In Section 6, the results and limitations of the study are presented and discussed. Finally, Section 7 draws conclusions based on the case study.

2. Literature Review

This section identifies the critical parameters related to this paper and discusses how these parameters are dealt with in the literature. A variety of signal patterns and their performance are also described. Furthermore, this section reviews how the performances of signal patterns are compared in the literature. In particular, Section 2.1 reviews the literature related to signal patterns while Section 2.2 reviews performance indicators such as Delay time, Potential Conflict, and Delay and Safety index. Finally, Section 2.3 focuses on the literature comparing signal pattern performance.

2.1. Signal Patterns

As previously mentioned, our aim in this paper is to preform comparisons of several signal patterns. Formally, a signal pattern dictates the possible user movements that are permitted during the green interval of a phase (a phase consists of a set of green, red, and clearance intervals assigned to specified traffic movement(s) during each cycle) [18]. In a typical four-leg (two-phase) intersection, we have four possible signal pattern types:

- Free pattern: no movement restrictions are applied to any phases during the green interval.
- Exclusive pattern: the green interval is partitioned into mutually exclusive (groups of) movements.
- Leading pattern: a group of movements is permitted for the complete green interval duration, while a second restricted group of movements is only permitted after a specific time interval.
- Lagging pattern: this pattern is similar to the leading ones, but the restricted movement group is only allowed before a specific time interval.

These patterns can be applied to the movements of each user category, but this study focuses on signal patterns that also explicitly account for pedestrian movements. The most common signal patterns that address the pedestrian interval are [18,19]:

- TWC (Two-Way Crossing): allows pedestrians to cross the intersection during the full duration of the green interval of the adjacent vehicular movement;
- EPP (Exclusive Pedestrian Phase): protects and excludes the pedestrian phase from all vehicular movements;
- LPI (Leading/Lagging Pedestrian Interval): leads or lags the green pedestrian interval, during which vehicles are not permitted to cross;
- LTI (Leading/Lagging Through Interval): similarly to LPI, it leads or lags the pedestrian interval; however, only vehicular turning movements are prohibited on a pedestrian green interval.

Given that LTI allows vehicles to cross the intersection during the green pedestrian interval, it is commonly preferred to LPI. For this reason, the present study focuses on the LTI, TWC, and EPP patterns, and it will not investigate the LPI pattern in depth.

2.2. Performance Indicators

In the literature, several indicators are developed to assess the performance of traffic signal; these indicators include the delay time [3,7], the traffic capacity [3], the system throughput [3,7], the intersection safety [2,4], the GHG emission count [2], the queue length [5], the travel time [5,6], etc. However, all these indicators are driven by two fundamental measures: the delay time (i.e., the additional travel time experienced by users compared to free movement through the intersection) and intersection safety (i.e., events to do with any conflict situations or possible interactions between vehicle and vehicle or pedestrian movements at the intersection). Therefore, our literature review focuses on these measures. We observe that these two measures are not entirely independent since a

lower level of safety corresponds to a higher level of potential conflict, and this can in turn impact the delay time. For this reason, we also review a third performance indicator called the Delay and Safety index, which provides the level of service of users at a signalized intersection by combining both pedestrian and vehicle delay and safety (represented by the number of users with potential conflicts). These three performance indicators are presented in Sections 2.2.1, 2.2.2 and 2.2.3, respectively.

2.2.1. Delay Time

As previously mentioned, the delay time at the intersection represents additional travel time experienced by users because of the traffic control system, changes in speed due to geometric conditions, incidents, and interactions with other road users versus free movement through the intersection [1]. While the delay time can generally account for several types of users, such as private vehicles, pedestrians, bikes, transits, we focus here on two aggregate user types: vehicles (including private and transit vehicles and bikes) and pedestrians.

Delay can be estimated using different models. As reported by [20], there are four primary methods for estimating the delay time: Akcelik [21], HCM [1], Webster [22], and HSL [20,23]. Among these models, the HCM is reputed to be more accurate even in situations with under or over-saturated intersections [24]. As mentioned earlier, one component of intersection delay is the vehicular delay. Equation (1) describes the vehicle delay model of HCM:

$$d^{veh} = d^U + d^I + d^Q \quad (s/veh) \tag{1}$$

where d^U defines the uniform delay based on the assumption of uniform arrivals and stable flow of vehicles; d^I defines the incremental delay due to the effect of random, cycle-by-cycle fluctuations in demand, which occasionally exceed capacity and are caused by a sustained oversaturation during the analysis period; and d^Q defines the initial queue delay resulting from unmet demand in the previous period. HCM refers to the saturation flow rate used to compute d^{veh} for different signal patterns, and can be calculated for each approach, lane, and movement group of the intersection [1].

The other component of the intersection delay is the pedestrian delay. Different studies modify the HCM model to include the pedestrian flow rate, pedestrian violation behavior, and traffic signal pattern [11,25,26]. The model proposed by [11,25] modifies the HCM to account for the pedestrian delay in TWC and EPP. This model comprises three parts. The first part is the signal delay (d^{sig}), defined as the waiting time of pedestrians stopping at the intersection because of the traffic light. The second part is the conflict delay (d^{con}), defined as the additional experienced delay time due to conflicts between pedestrians and turning vehicles. The third part is the detour delay (d^{det}) due to the fact that pedestrians willing to cross the intersection diagonally must perform a detour if the considered signal pattern does not allow diagonal crossing. As a consequence, Ma et al. (2015) [11] determine the average pedestrian delay time as:

$$d^{ped} = d^{sig} + d^{con} + d^{det} \quad (s/ped) \tag{2}$$

where d^{ped} and d^{veh} are the average per-user delay of pedestrians and vehicles, respectively. Ma et al. (2014) [25] recommend adapting the weighted delay as the intersection delay (s/user):

$$D = \frac{d^{veh}V^{veh} + d^{ped}V^{ped}}{V^{veh} + V^{ped}} \quad (s/user) \tag{3}$$

where V^{veh} and V^{ped} refer to the vehicle volume and pedestrian volume of the intersection, respectively.

We observe that expressions of both the vehicle delay in the HCM model and the pedestrian delay proposed in Ma et al. (2014) [25] depend on the specific pattern to which the measure is applied. For this reason, in the rest of the paper, we add a superscript p with $p \in \{TWC, LTI, EPP\}$ to underline such a dependence when needed. For example we use

D^p to denote the weighted intersection delay time for pattern p; similarly, we use d^{veh-p} and d^{ped-p}, for the vehicle delay and pedestrian delay for pattern p.

The vehicle delay HCM model is based on the saturation flow rate of each movement group. Therefore, Equation (1) will be applied for computing d^{veh-p} for $p \in \{TWC, LTI, EPP\}$ in our study. However, d^{ped-p} has not been fully investigated in the literature. We will address this gap in Section 4 of this study.

2.2.2. Potential Conflict

Intersection safety is defined as the number of potential vehicle-to-vehicle and vehicle-to-pedestrian conflict situations at the intersection. A conflict is any possible unsafe situation or interaction between user movements at the intersection. A conflict with high severity is usually known as a collision and crash [27].

Different elements are used to predict or analyze the safety level of intersections based on crash history data. These factors include the severity classification, the post-encroachment time, the time-to-collision [28], the average daily traffic and accident modification factor [14], the time to collision [29]), the annual average daily traffic [13], the average hourly conflict, the square root of users volume at the intersection, and the intersection conflict index [15,30]. Most of these factors are suitable for measuring the vehicle-to-vehicle conflict. To quantify pedestrian-to-vehicle conflict risk, some authors applied indices such as pedestrian level of comfort, pedestrian level of stress, and pedestrian intersection index, which are related to the pedestrian comfort at the intersection, intersection geometry, daily user volume, and the user speed [31]. These indices are useful for comparing the level of pedestrian safety at different intersections. However, the value of these indices would not change with the signal pattern of the intersection. Therefore, to grasp the influence of the traffic signal pattern on pedestrian safety, another index needs to be developed.

Zhang et al. (2003) [32], based on HCM, proposed the Potential user Conflict (PC) metric, which is intended to provide a measure of the degree of safety at the intersection and indicates the frequency of unsafe (conflict) situations. This measure can be applied to pedestrian and vehicle conflicts for an individual intersection based on the traffic flow and signal pattern [32]. They focused on an intersection with shared, permitted, and protected left turn movement scenarios. Equation (4) defines the potential conflict (number of users in conflict/interval) as provided by [32]:

$$PC = pc^{v2v} + pc^{v2p} \quad (user\ with\ conflict\ /time\ interval) \tag{4}$$

where pc^{v2v} represents the total number of vehicles with a potential conflict (v2v) for each time interval and pc^{v2p} is the total number of pedestrians with a potential conflict with vehicle (v2p) for each time interval. PC model of Zhang et al. (2003) [32] computes the number of conflicts for each group of movements based on their interaction with another group of movements for the specific period. Therefore, the model can be defined for each pattern studied. In the rest of the paper, we use the sum of the number of vehicles with a potential vehicle-to-vehicle conflict pc^{v2v-p}, and the number of pedestrians with a potential conflict with vehicle pc^{v2p-p} for each pattern $p \in \{TWC, LTI, EPP\}$ with PC^p to denote the total number of users with potential conflicts for each time interval.

2.2.3. Delay and Safety Index

Zhang et al. (2003) [32] introduced an indicator called the Delay and Safety index (DS) for use in comparing different patterns. DS (s/user) indicator reflects the combined effects of delay and potential conflict situations for pedestrians and vehicles. Equations (5) and (6) define the vehicle Delay and Safety index (DS^{veh}) and the pedestrian Delay and Safety index (DS^{ped}), respectively.

$$DS^{veh} = d^{veh} \left(1 + pc^{v2v}/V^{veh}\right) \quad (s/veh) \tag{5}$$

$$DS^{ped} = d^{ped} \left(1 + pc^{v2p}/V^{ped}\right) \quad (s/ped) \tag{6}$$

where d^{veh} and d^{ped} denote the average vehicle and pedestrian delay, respectively, and V^{veh} and V^{ped} denote the vehicle and pedestrian volumes of the intersection for a given reference time interval, respectively. We observe that DS index is a measure of the level of service at the intersection that accounts for both delay time and potential conflicts. Zhang et al. (2003) [32] proposed to integrate Equations (5) and (6) into a single weighted expression as:

$$DS = \frac{DS^{veh}\,V^{veh} + DS^{ped}\,V^{ped}}{V^{veh} + V^{ped}} \quad (s/user). \tag{7}$$

This model is based on the number of users with potential conflicts and the average user delay and can be specified for each signal pattern. Therefore, we can modify DS model for pattern $p \in \{TWC, LTI, EPP\}$ and we define DS^p, DS^{veh-p} and DS^{ped-p} as the Delay and Safety index, the vehicle Delay and Safety index, and the pedestrian Delay and Safety index for patterns $p \in \{TWC, LTI, EPP\}$, respectively.

2.3. Comparison of Signal Patterns

In Section 2.1, we defined the signal pattern as a set of movements that users are allowed to perform during the green interval of a phase in each cycle. The literature reports that the signal pattern with leading, lagging, or separating intervals can improve the travel experience quality at the intersection by influencing both the delay and safety [19,33–35]. Some studies have compared these patterns in terms of their cycle length, delay time, and safety [7,10]. As mentioned in Section 2.2, we consider D, PC, and DS as reliable and measurable performance indicators that can be used to compare the level of service of each signal pattern for a specific intersection.

Section 2.1 considers that the most common signal patterns accounting for both vehicles and pedestrians are EPP (Exclusive Pedestrian Phase), TWC (Two-Way Crossing), and LTI (Leading Through Interval). The literature compares these patterns by analyzing how they affect delay time and safety under various user volumes. For example, a comparison between EPP and TWC using different traffic data shows that EPP in an intersection with a low pedestrian volume increases the delay at the intersection and causes violation behavior among pedestrians, which consequently leads to reduced intersection safety [9–11]. TWC with a high volume of pedestrians and (right or left) turning vehicles can increase the number of conflict situations [10].

LTI minimizes conflicts between pedestrians and vehicles without significantly impacting vehicular movement. However, separating the turning and through lanes at each approach is necessary; otherwise, vehicle delay increases at the intersection [36]. Furthermore, patterns with exclusive intervals (LTI and EPP) at an intersection with low pedestrian volumes can increase delays. However, it is expected that EPP will increase the delay significantly since it stops vehicular movements and forces pedestrian movements for exclusive intervals, and will increase the cycle length to reduce the capacity ratio of the intersection [19].

Besides looking at the literature that compares the results of different patterns while the traffic signal performs the fixed pattern for the entire period covered by the study, we aim to study how allowing the signal pattern to change dynamically during operations according to observed traffic demand can potentially impact the traffic signal performance. Unlike what is largely observed in the literature, with traffic signal performance based exclusively on vehicle-related measures, this study aims to include pedestrian-related parameters. Delay time, potential conflicts and their combination are among the most widely adapted performance indicators in the literature. Section 3 provides the methodology of our study which investigates how traffic signal efficiency is affected by dynamically changing signal patterns.

3. Materials and Methods

The methodological approach adopted for the present study differs from existing methods in several ways. First, the study focuses on adapting a performance indicator

model to suit different pedestrian related signal patterns. Second, it simulates real-time data of pedestrians and vehicles throughout the day. Thirdly, it compares different signal patterns based on performance indicators to provide the best performing pattern for each study period. Moreover, it investigates how dynamic signal patterns (hybrid patterns) can improve service levels.

To address the three research objectives identified in Section 1, we proceed in three stages:

- First, delay and potential conflict parameters of each studied pattern are modified in Section 4 (see Table 3).
- Then, the studied patterns are investigated through a case study. They are simulated based on observed demand, and D, PC and DS are computed for each pattern in Section 5.
- Finally, the performance of each pattern in the case study is compared for every time step. Following this comparison, a hybrid pattern maximizing the service level over the entire study period is developed and its performance is compared to that of other patterns in Section 5.

As discussed in Section 2, the equations used in this study are developed based on the HCM. The first stage of our methodology consists in modifying the equations for each studied signal pattern and using the HCM approach to ensure that the performance indicator is pedestrian-sensitive. Therefore, D, PC, and DS equations developed in Sections 4.1, 4.2 and 4.3, respectively, comply with the HCM, 6th edition.

In the second stage of the approach, a case study is developed, and focuses on an isolated intersection with an average volume of 3660 users per hour for the day of study. The case study is selected by choosing a signalized intersection: (1) having the characteristics of a single and isolated intersection, (2) with a demand volume varying throughout a typical working day, and (3) for which real-time traffic data can be extracted. Following the HCM approach, demand data are obtained at regular intervals (15 min) and for all users.

In this second stage, Synchro version 10 is selected to simulate the traffic data because: (1) it allows calculations based on the 6th edition of HCM, (2) it is flexible enough to simulate the signal patterns investigated in this study, and (3) it is freely available to the authors. According to Cubic (2019), "Synchro Software and its suite of associated applications is a traffic signal timing software that assists engineers and transportation planners design, model, optimize, simulate and animate signalized and unsignalized intersections" [37]. Synchro simulates each study period based on the real-time data of the case study intersection to provide the optimum cycle length, green time, and vehicle delay for each pattern. Synchro's ring-barrier option enables the user to define the traffic pattern to be simulated, while Synchro optimizes the length of each phase. Moreover, the performance, in terms of factors such as vehicle delay, traffic signal cycle length, and green time, is extracted directly from simulation results. The HCM and Synchro consider the saturation flow rate of the movement group in computing the vehicular delay for each signal pattern. Therefore, we use Synchro's estimation of vehicular delay in our study. Following HCM 6th edition, and to ensure results accuracy, Synchro simulates the traffic signal for each 15-min interval.

To assess the impact of the cycle length on the performance of each signal pattern, two sets of simulations are run. First, the green phase and vehicular delay are extracted from Synchro for different fixed cycle length values, and second, the cycle length, green time of each phase, and vehicular delay are optimized by Synchro, from which they are then extracted. For each studied pattern, the pedestrian delay and conflict situations are then calculated based on the equations in Section 4.

The next methodological stage consists of a comparison of the performance indicator values obtained from the signal patterns according to the equations in Section 4 to identify the best performing pattern (the pattern that most improves the level of service) for every 15 min. We investigate and simulate three patterns (LTI, TWC, EPP) and build a hybrid pattern, consisting of a pooling of the best performing pattern for each interval. Finally, for each performance indicator, we compare the performance of the hybrid pattern to that of

the three regular patterns (LTI, TWC, EPP) to verify whether the hybrid pattern improves the performance indicators.

4. Development of Pedestrian-Sensitive Performance Indicators

The performance indicators mentioned in Section 2 are not available for all patterns, and do not generally consider signal patterns with both pedestrian- and vehicle-sensitive indicators. The performance indicators used in this paper adapt the state-of-the-art indicators to all signal patterns considered (i.e., TWC, EPP, LTI) and generalize the indicators to account for pedestrians and vehicles.

This paper proposes a new delay measure by building on the model of Ma et al. (2015) [11], introduced in Section 2.2.1, which suitably accounts for pedestrians. It also modifies the potential conflict and delay and safety models proposed by Zhang (2003) [32] to cover all signal patterns of our study. These models are introduced in Sections 2.2.2 and 2.2.3, respectively.

The resulting pedestrian models, namely, the conflict model and the delay and safety model, are presented in Sections 4.1, 4.2 and 4.3, respectively.

4.1. Computation of the Delay Time for Each Signal Pattern

In this study, the intersection delay is considered as a weighted average of pedestrian and vehicle delays. Since the pedestrian delay of Ma et al. (2015) [11] only considered TWC and EPP, we further develop their delay model to also consider the LTI pattern by modifying the delay time model described by Equation (2) for the regular four-arm intersection. Figure 1 illustrates the four-arm intersection layout as a reference intersection model for this study. The set, parameters and variables used to compute the pedestrian delay are described in Table 1.
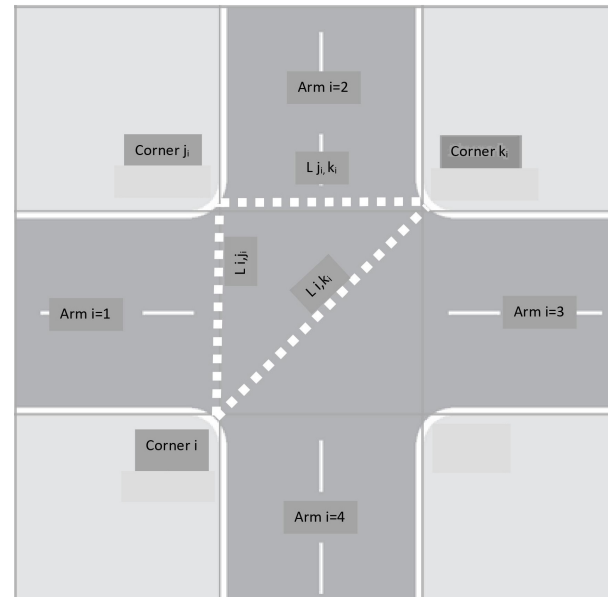

Figure 1. Reference intersection layout with key parameters used in the simulation.

Table 1. Sets, parameters and descriptions.

Sets, Parameters, Variables	Description	Value Obtained From
$i \in I = \{1, 2, 3, 4\}$	Set of arms and corresponding corners at an intersection	–
$j_i \in I$	Arm and corner following $i \in I$ $$j_i = \begin{cases} i+1 & i \leq 3 \\ 1 & otherwise \end{cases}, \forall i \in I$$	–
$k_i \in I$	Diagonal corner from corner $i \in I$, $$k_i = \begin{cases} i+2 & i+2 \leq 4 \\ (i+2)-4 & otherwise \end{cases}, \forall i \in I$$	–
g_i^{veh}	Duration of green for vehicles from arm $i \in I$, (s)	Simulation (Synchro)
g_i^{ped}	Duration of green for pedestrian crossing arm $i \in I$, (s)	Simulation (Synchro)
l_{ij_i}	Length of crosswalk from corner i to corner j_i, (m)	Observation
v^{ped}	Average walking speed of pedestrians, (m/s)	Observation
α_{ik_i}	Portion of pedestrian volume from corner i to corner k_i in total pedestrian demand of corner $i \in I$	Observation
t	Acceptable gap: time between vehicles when the vehicle confidently does (a) lane change(s)	Computation
μ_i	Flow rate of vehicles turning on corner $i \in I$ (veh/h)	Observation
C	Cycle length,(s)	Simulation (Synchro)
d^{ped}	Pedestrian delay at intersection(s)	Computation
d^{sig}	Pedestrian delay due to traffic signal at crosswalk(s)	Computation
d^{con}	Pedestrian delay due to conflicts with turning vehicles(s)	Computation
v_i^{lt}	Number of left turning vehicles on approach $i \in I$ during green interval of g_q	Observation
v_i^{ot}	Number of vehicles moving in the opposite direction on approach i during green interval of g_u	Observation
d^{det}	Pedestrian delay due to detour distance(s)	Computation

As mentioned in Section 2.2.1, the three parts constituting the pedestrian delay in Equation (2) are calculated by Equations (9)–(11) [11]:

$$d^{ped} = d^{sig} + d^{con} + d^{det} \quad (s/ped) \tag{8}$$

where d^{ped} is the average pedestrian delay at the intersection; d^{sig} is the pedestrian delay due to the traffic signal at the crosswalk; d^{con} is the pedestrian delay due to conflicts with turning vehicles; and d^{det} is the pedestrian delay due to detour distance, which is defined as the difference between the time needed by pedestrians to cross diagonally to corner k_i and the time to cross conventionally from corner i to j_i and then from j_i to k_i.

The pedestrian signal delay is defined as a waiting time due to the red interval of a traffic signal, and was introduced by Ma et al. (2015) [11] as Equation (9):

$$d^{sig} = \sum_{i \in I} \left(\frac{(C - g_i^{ped})^2}{2C} + \alpha_{ik_i} \frac{(g_i^{veh} - \frac{l_i}{v_i^{ped}})(C - g_i^{ped}) + 0.5 g_{j_i}^{ped} (g_{j_i}^{veh} - \frac{l_{j_i}}{v_{j_i}^{ped}})}{C} \right) \quad (s/ped) \tag{9}$$

The first part of Equation (9) calculates the pedestrian signal delay for a pedestrian intending to cross from arm i to arm j_i (conventionally). The second part of Equation (9) measures the pedestrian waiting time to cross diagonally from corner i to corner k_i. How-

ever, because of traffic light patterns, pedestrians have to cross from corner i to j_i and stop for the pedestrian green interval of arm $i + 1$, and then cross from corner j_i to k_i.

The pedestrian conflict delay was defined in the model of Ma et al. (2015) [11] as Equation (10):

$$d^{con} = \sum_{i \in I} \left(\frac{e^{\mu_i t} - \mu_i t - 1}{\mu_i} + a_{ik_i} \frac{e^{\mu_{j_i} t} - \mu_{j_i} t - 1}{\mu_{j_i}} \right) \quad (s/ped) \tag{10}$$

where d^{con} is recalculated as a result of the interaction between pedestrians and vehicles, related to the volume of turning vehicles and gap time between vehicles at arm i. Equation (10) is also divided into two parts. The first covers pedestrians crossing from corner i to corner j_i, and the second is related to pedestrians intending to cross from corner i to k_i. The latter may experience interactions with vehicles at corner j_i.

The last part of the pedestrian delay in the model of [11] is the detour delay. This delay is related to the length of the crosswalk and the pedestrian speed. It is the difference between the time required for a pedestrian intending to cross the intersection diagonally to cross the intersection conventionally (i.e., one approach after the other) as compared to diagonally. The detour delay is defined as follows:

$$d^{det} = \sum_{i \in I} \frac{l_{ij_i} + l_{j_i k_i} - l_{ik_i}}{v^{ped}} \quad (s/ped) \tag{11}$$

We adapt Equations (9)–(11) to define the pedestrian delay for TWC, EPP, and LTI.

User movements under a typical TWC phase at a four-approach intersection are shown in Figure 2. In TWC, pedestrians cannot cross the intersection directly from corner i to corner k_i. First, they have to cross from corner i to j_i, and then from corner j_i to k_i. Therefore, the pedestrian delay for TWC includes a detour delay and both the first and second parts of a signal delay and a conflict delay. The pedestrian delay in TWC is defined as follows:

$$d^{ped-TWC} = d^{sig} + d^{con} + d^{det} \quad (s/ped), \tag{12}$$

where $d^{ped-TWC}$ is calculated with Equation (2).
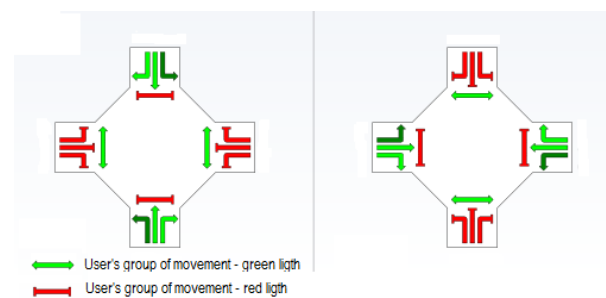
Figure 2. Typical TWC phase diagram for a four-arm intersection.

The EPP pattern allows pedestrians to cross the intersection conventionally or diagonally without interaction with turning vehicles. Therefore, the study only expects the first part of d^{sig} in Equation (9) to be applied for pedestrians coming to the intersection during the "do not walk" or "stop" intervals of the pedestrian light. Figure 3 shows that all vehicle movements are stopped at the intersection under the EPP pattern; therefore, the conflict delay and the detour delay are not applied for this pattern. Equation (13) defines the EPP pedestrian delay as:

$$d^{ped-EPP} = d^{sig-EPP} \quad (s/ped) \tag{13}$$

where the pedestrian delay of the exclusive pedestrian pattern ($d^{ped-EPP}$) only includes the signal delay defined as:

$$d^{sig-EPP} = \sum_{i \in I} \frac{(C - g_i^{ped})^2}{2\,C} \qquad (s/ped) \tag{14}$$
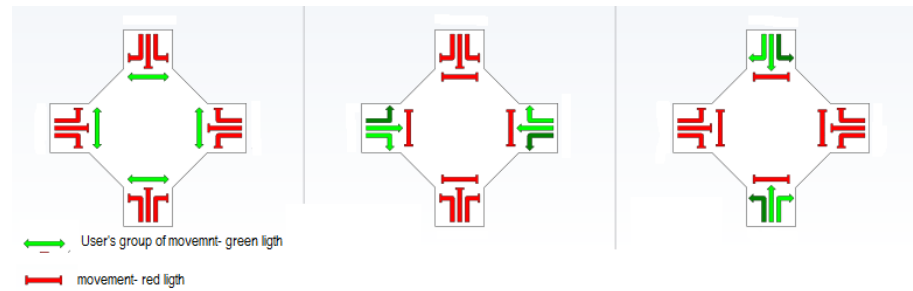

Figure 3. Typical EPP phase diagram for a four-arm intersection.

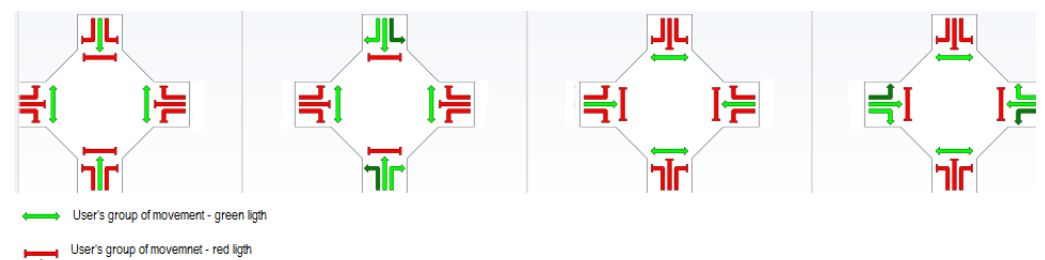Figure 4 presents the typical LTI phase diagram at the intersection with four approaches:

Figure 4. Typical LTI phase diagram for a four-arm intersection.

LTI assumes that pedestrians cross the street only during the "walk" interval and does not consider any pedestrian violation behavior. In the LTI pattern, the green interval for turning vehicles starts while pedestrians are in the "do not walk" interval. Therefore, the study does not expect any pedestrian conflict delay for this pattern; as well, d^{sig} and d^{det} are calculated with Equations (9) and (11), respectively. The LTI pedestrian delay is then defined as follows:

$$d^{ped-LTI} = d^{sig} + d^{det} \qquad (s/ped) \tag{15}$$

Therefore, we modified d^{ped} according to each signal pattern of the study; in the next section, we modify the conflict-related equations for each signal pattern. As we discussed in Section 2.2.1, we respect the HCM vehicular delay model since it reflects each pattern by considering the saturation flow rate of the group of movements for each lane. Then, we compute the intersection delay (D) according to Equation (3) for each study pattern.

4.2. Computation of the Potential Conflict for Each Signal Pattern

Table 2 lists the parameters and variables for the intersection depicted in Figure 1 that are needed to compute pc^{v2v} and pc^{v2p}.

The number of potential conflicts between vehicles caused by left-turning vehicles at the intersection is defined as follows [32]:

$$pc^{v2v} = \sum_{i \in I} (pc_i^{lt} + pc_i^{ot}) \qquad (vehicle\ with\ conflict/time\ interval) \tag{16}$$

where pc_i^{lt} is equal to pc_i^{ot} if the conditions of Equation (17) are valid:

$$pc_i^{lt} = pc_i^{ot} = \begin{cases} v_i^{lt}\, p_i^{pc} & if\ v_i^{lt} \leq v_i^{ot} \\ v_i^{ot}\, p_i^{pc} & if\ v_i^{lt} > v_i^{ot} \end{cases} \quad \forall\, i \in \{1, 2, 3, 4\} \tag{17}$$

Equation (17) considers that $pc_i^{lt} = pc_i^{ot}$ at the specific condition related to v^{ot} and v^{lt} on the green interval of g^u, while g^u is defined as Equation (18):

$$g^u = \begin{cases} g - g^o & if\ g^o \geq g^f \\ g - g^f & if\ g^o < g^f \end{cases} \quad \forall\, i \in \{1, 2, 3, 4\} \tag{18}$$

where g^f is the part of the green time (g) before the first turning vehicle arrives at the intersection and g^o is the part of the green time while left-turning vehicles have to stop until opposing through queue of vehicles is cleared up.

Table 2. Sets, parameters, variables and descriptions.

Sets, Parameters, Variables	Description	Value Obtained From
$i \in I = \{1, 2, 3, 4\}$	Set of approaches at intersection	–
v_i^{lt}	Number of left-turning vehicles on approach $i \in I$ during the green interval of g_q	Observation
v_i^{ot}	Number of vehicles moving in the opposite direction on approach i during the green interval of g_u	Observation
p_i^{pc}	Probability of potential left turn conflict on approach $i \in I$	Computation
v^{ped}	Pedestrian flow rate in the subject crossing (walking in both directions) (ped/h)	Observation
g^{ped}	Pedestrian service time(s)	Simulation (Synchro)
g^{veh}	Vehicle service time(s)	Simulation (Synchro)
g^q	Amount of permitted green time that is not blocked by (an) opposing lane(s)	Observation
occ^l	Relevant conflict zone occupancy for conflicts between permitted or protected left-turning vehicles and pedestrians	Computation
v^o	Opposing demand flow rate (veh/h)	Observation
g^{pl}	Effective green time for permitted left turn operation(s)	Observation
t^c	Critical gap(s)	Computation
V^{veh}	Total vehicle volume (veh/h)	Observation
V^{ped}	Total pedestrian volume (ped/h)	Observation
pc^{v2v}	Total expected number of vehicles with potential conflicts (veh/interval)	
pc^{v2p}	Total expected number of vehicles with potential conflicts (veh/time interval)	Computation
pc_i^{lt}	Number of left-turning vehicles with potential conflicts on approach $i \in I$	Computation
pc_i^{ot}	Potential conflicts of opposing vehicles resulting from left turn on approach $i \in I$	Computation
occ^{ped-g}	Pedestrian occupancy	Computation
occ^r	Relevant conflict zone occupancy for conflicts between right-turning vehicles and pedestrians	Computation
g^f	Part of green time (g) before the first turning vehicle arrives at the intersection(s)	Observation
g^o	Part of the green time while left-turning vehicles stop to opposing through queue of vehicles get clear(s)	Observation
g^u	Portion of green time during which there is no potential conflict between left-turning and through vehicle(s)	Observation
v^{ped-g}	Pedestrian flow rate during pedestrian service time	Computation
occ^{ped-u}	Pedestrian occupancy when the opposing queue is clear	Computation

Zhang et al. (2003) [32] considered that left-turning vehicles do not get into conflict with vehicles moving through in the following circumstances:

- At the beginning of the green interval, when the turning vehicle has to stop for the through vehicles, and then there is no conflict.

- When the gap between the vehicles in through movement is less than 4 s, the driver cannot make a left turn.
- When the gap between vehicles' through movement is more than 8 s, the driver has enough time to make a left turn, and there is no conflict.

For left turn situations that are not included above, Zhang et al. (2003) [32] defines the probability of a potential left turn conflict (p^{pc}) on each approach based on the turning time and turning distance for left-turning vehicles when the gap time for through vehicles is between 4 and 8 s. In the case of the LTI pattern, g^f is zero because there is already an accumulation of left-turning vehicles during the late start of the green interval. Then, g^u of LTI is defined as:

$$g^u = g - g^o \qquad \forall\, i \in \{1, 2, 3, 4\} \tag{19}$$

Regarding Equations (16) and (18), pc^{v2v} is related to the number of vehicles and the effective green interval for the left-turning vehicles.

Besides Equation (16), which computes pc^{v2v} based on the traffic flow rate and to estimate pc^{v2v}, Zhang et al. (2003) [32] proposed the following model based on the conflict zone occupancy at the intersection for pedestrian and turning vehicles:

$$v^{ped-g} = v^{ped}\left(C/g^{ped}\right) \tag{20}$$

where v^{ped-g} is the pedestrian flow rate during the pedestrian service time. The authors used Equation (20) to define the pedestrian occupancy at the intersection based on the pedestrian flow rate, as shown in Equations (21) and (22):

$$occ^{ped-g} = v^{ped-g}/2000 \qquad If\ v^{ped-g} \le 1000 \quad (ped/h) \tag{21}$$

$$occ^{ped-g} = 0.4 + (v^{ped-g}/10000\ ) \qquad If\ v^{ped-g} > 1000 \quad (ped/h) \tag{22}$$

Depending on the pedestrian flow rate, occ^{ped-g} is calculated by Equations (21) or (22), and then the number of conflict situations between pedestrians and right-turning vehicles at the intersections is introduced in the literature as Equation (23):

$$occ^r = \frac{g^{ped}}{g^{veh}}\, occ^{ped-g}, \tag{23}$$

where occ^r defines the number of pedestrian conflicts with right-turning vehicles related to pedestrian occupancy and the green interval of the traffic signal.

To compute the number of pedestrian conflicts with left-turning vehicles, the previous literature presented the pedestrian occupancy when the opposing queue is clear:

$$occ^{ped-u} = (1 - \frac{0.5\, g^q}{g^{ped}})\, occ^{ped-g} \tag{24}$$

If $g^q < g^{ped}$, then Equation (24) is applied to calculate occ^{ped-u}; otherwise, $occ^{ped-u} = 0$. Equations (25) or (26) define the conflict between pedestrians and left-turning vehicles.

$$occ_l = \frac{g^{ped} - g^q}{g^{pl} - g^q}\, occ^{ped-g}\, e^{-t_c\ (v^o/3600)} \tag{25}$$

Then, Zhang et al. (2003) [32] defined pc^{v2p} as:

$$pc^{v2p} = \sum_{i \in I}(v_i^{ped}\, occ_i^r\,) \quad (pedestrian\ with\ conflict/time\ interval) \tag{26}$$

They also considered *PC* at the intersection as a sum of pc^{v2v} and pc^{v2p} for each period of the study, as presented in Equation (27):

$$PC = pc^{v2v} + pc^{v2p} \quad (user\ with\ conflict/time\ interval) \tag{27}$$

Zhang et al. (2003) [32] did not provide the *PC* models for the specific pattern of our study, but only investigated the effect of shared, protected, and permitted vehicle left turn movements. For the present study, *PC* models of Zhang et al. (2003) [32] as presented in Equation (16) to Equation (27) were modified for each signal pattern, considering the logic of relevant conflict movements. For example, pc^{v2p} is not applied to the EPP pattern since there is no vehicle-pedestrian interaction in this pattern. Therefore, Equations (28) and (29) describe the potential pedestrian conflict for TWC and LTI patterns based on pedestrian conflict with left- and right-turning vehicles (Equations (23) and (25)):

$$pc^{v2p-TWC} = \sum_{i \in I}(v_i^{ped} \, occ_i^r + v_i^{ped} \, occ_i^{ped-u}) \quad (\textit{pedestrian with conflict/time interval}) \tag{28}$$

$$pc^{v2p-LTI} = \sum_{i \in I}(v_i^{ped} \, occ_i^r + v_i^{ped} \, occ^l) \quad (\textit{pedestrian with conflict/time interval}) \tag{29}$$

The only difference between these two equations is related to pedestrian interference with left-turning vehicles. Following Equation (4), Equations (30)–(32) define the total expected potential conflicts at the intersection for each pattern as the sum of the total expected number of potential conflicts between vehicles (pc^{v2v}) (Equation (16)), and the total expected potential pedestrian conflicts (pc^{v2p-p}) (Equation (28) or (29)).

$$PC^{TWC} = \; pc^{v2v} + pc^{v2p-TWC} \quad (\textit{user with conflict/time interval}) \tag{30}$$

$$PC^{LTI} = \; pc^{v2v} + pc^{v2p-LTI} \quad (\textit{user with conflict/time interval}) \tag{31}$$

$$PC^{EPP} = \; pc^{v2v} \quad (\textit{user with conflict/time interval}) \tag{32}$$

It should be noted that the value of the potential conflict related to each signal pattern (PC^p) depends on pc^{v2p-p} only since pc^{v2v} does not vary with the traffic signal pattern. Zhang et al. (2003) [32] computed *PC* as an hourly number of potential conflicts, considering the hourly volume and green interval of the traffic signal. The models used in the present study are based on 15-min intervals, and therefore, *PC* refers to the number of potential conflicts for every 15 min herein.

4.3. Computation of the Delay and Safety Index for Each Signal Pattern

Delay and safety index (*DS*) values show the effect of different signal patterns on the level of service. *DS*, as defined in Equation (7), must be adapted for signal pattern $p \in \{TWC, LTI, EPP\}$ by considering pc^{v2v-p}, pc^{v2p-p}, d^{veh-p} and d^{ped-p}. Equation (33) describes DS^p:

$$DS^p = \frac{DS^{veh-p} \, V^{veh} + DS^{ped-p} \, V^{ped}}{V^{veh} + V^{ped}} \quad (s/user) \tag{33}$$

where DS^{veh-p} and DS^{ped-p} define *DS* of the vehicle and *DS* of pedestrian for pattern $p \in \{TWC, LTI, EPP\}$.

As mentioned in Section 4.2, pc^{v2v} is not dependent on the signal pattern, whereas the vehicle delay varies for each signal pattern. Since Zhang et al. (2003) [32] do not investigated *DS* according to the signal pattern, we modify Equations (5) and (6) to take into account DS^{veh-p} and DS^{ped-p} in Equations (34) and (35):

$$DS^{veh-p} = d^{veh-p} \, (1 + \frac{pc^{v2v}}{V^{veh}}) \quad (s/veh) \tag{34}$$

$$DS^{ped-p} = d^{ped-p} \, (1 + \frac{pc^{v2p-p}}{V^{ped}}) \quad (s/ped) \tag{35}$$

where DS^{veh-p} and DS^{ped-p} respectively describe the level of service and safety for vehicles and pedestrians for each period of the study under each signal pattern $p \in \{TWC, LTI, EPP\}$. d^{veh-p} is extracted from Synchro based on Equation (7). d^{ped-p} are computed based on Equations (12), (13) and (15). pc^{v2v} is computed based on Equation (16) and pc^{v2p-p} is computing based on Equations (28) and (29). One of the goals of the present study is to identify the pattern with the minimum DS value that represents the best service and safety level for an intersection. Table 3 summarizes the equations related to the methods used to measure the delay and conflict developed in this section.

Table 3. Equations related to each pattern.

Pattern	D (s/User)	PC (User with Conflict/Interval)	DS (s/User)
TWC	$\frac{d^{veh}V^{veh}+(d^{sig}+d^{con}+d^{det})V^{ped}}{V^{veh}+V^{ped}}$	$pc^{v2v} + pc^{v2p-TWC}$	
EPP	$\frac{d^{veh}V^{veh}+(d^{sig-EPP})V^{ped}}{V^{veh}+V^{ped}}$	pc^{v2v}	$\frac{DS^{veh-p}\ V^{veh}+DS^{ped-p}\ V^{ped}}{V^{veh}+V^{ped}}$
LTI	$\frac{d^{veh}V^{veh}+(d^{sig}+d^{det})V^{ped}}{V^{veh}+V^{ped}}$	$pc^{v2v} + pc^{v2p-LTI}$	

In the following section, we investigate our performance for each pattern and look into whether it can be affected by dynamically changing the pattern during course of the day.

5. Case Study

This section describes the experimental campaign developed to dynamically assess the potential impact of allowing traffic system controls to change the pattern according to real-time traffic conditions. The experiment consists mainly of a computational case study where an existing traffic signal is selected and its performance is simulated under real-life traffic conditions. First, three patterns, namely, TWC, EPP and LTI, are simulated. Then, a hypothetical hybrid pattern is created by choosing, for each time interval, the best performing pattern associated with each performance indicator. For those simulations, two pre-defined cycle lengths are tested. We also investigate the optimum cycle length for each signal pattern. However, the optimum cycle length in Synchro seeks to minimize the delay time and does not consider safety in its objective function. Thus, we exclude the investigation of the signal patterns with the optimum cycle length from our study.

Section 5.1 describes the case study and the demand collection mechanism. Section 6 presents the computational results for the fixed cycle length experiments. Finally, Section 6.5 provides an in-depth discussion to validate the proposed model.

5.1. Description of the Case Study

The considered intersection is close to downtown Montreal (Notre-Dame and Peel Streets), with École de technologie supérieure (ÉTS) situated on both sides of its southern arm, and with one full day of data being available. In the present study, the intersection is considered as isolated (not coordinated with other intersections), and therefore, the target traffic signal runs in an uncoordinated semi-actuated mode. It is assumed that vehicles cannot turn right on red traffic signals, based on Montreal traffic rules.

Real traffic data are collected from the ÉTS security camera system for a regular day (Wednesday, 8 October 2018, from 8 a.m. to 8 p.m.). A video camera is installed on top of the ÉTS building to capture a full view of the intersection. A manual video imaging process is applied to manage the data collected from Notre-Dame and Peel (Figure 5). Detailed data on pedestrian and vehicle volumes and the traffic signal configuration associated with the intersection are also collected. The average pedestrian/vehicle flow rate at this intersection is approximately 900 users/15 min. The pattern currently applied to this intersection is the LTI.

Figure 5. Aerial view of the case study site–Notre-Dame and Peel intersection.

Figure 6 demonstrates the pedestrian and vehicle flow during the day. It shows that pedestrian traffic at the intersection experiences is at a peak at 8:45 a.m. (748 pedestrians/ 15 min), while for vehicles, it is at 5:30 p.m. (633 vehicles/15 min). Furthermore, pedestrians outnumber vehicles on three occasions during the day (8:30 a.m., 1:00 p.m., and 5:30 p.m.).
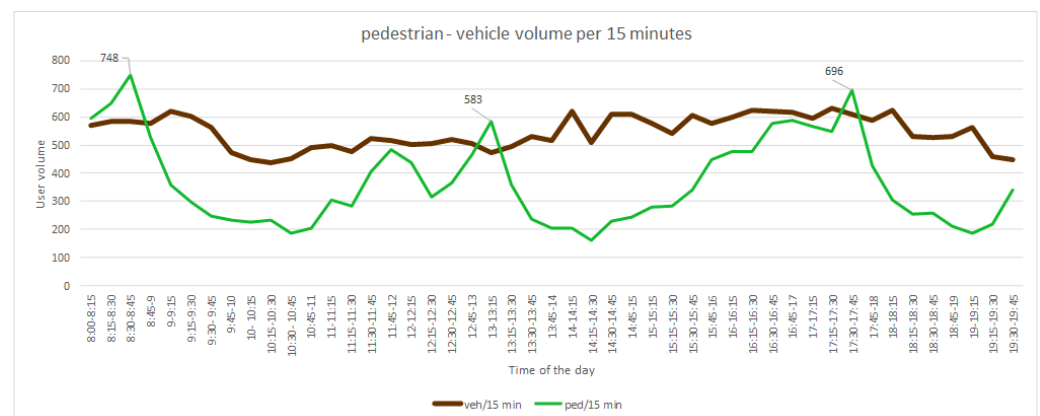

Figure 6. Pedestrian and vehicle volumes during course of the day for every 15 min.

The following section investigates the results for performance indicators when two fixed cycle lengths are applied to the case study data.

6. Results

We perform the case study using different fixed cycle lengths and investigate whether performance indicators can be improved by dynamically changing signal patterns. The current operational cycle length at the considered intersection is approximately 80 s. For this reason, we compare the patterns by assigning an 80-s fixed cycle length in the first experiment. Moreover, when the cycle lengths are 45 (minimum acceptable cycle length by Synchro) and 60 s, we simulate the data with Synchro. The case of a 45-s cycle length resulted in an over-saturated intersection and, as a result, we only focus on 60- and 80-s fixed cycle lengths. Synchro's ring-barrier option enables the simulation of different signal patterns, while the lane setting remains the same for all signal patterns. The input data are the pedestrian and vehicle volumes, lane group movements, and possible turning movements for each intersection approach. All other parameters are set at their Synchro default values. Figure 7 shows Synchro interface while it displays the results for the TWC pattern at 7:45 p.m., including the cycle length, delay, and phase duration.
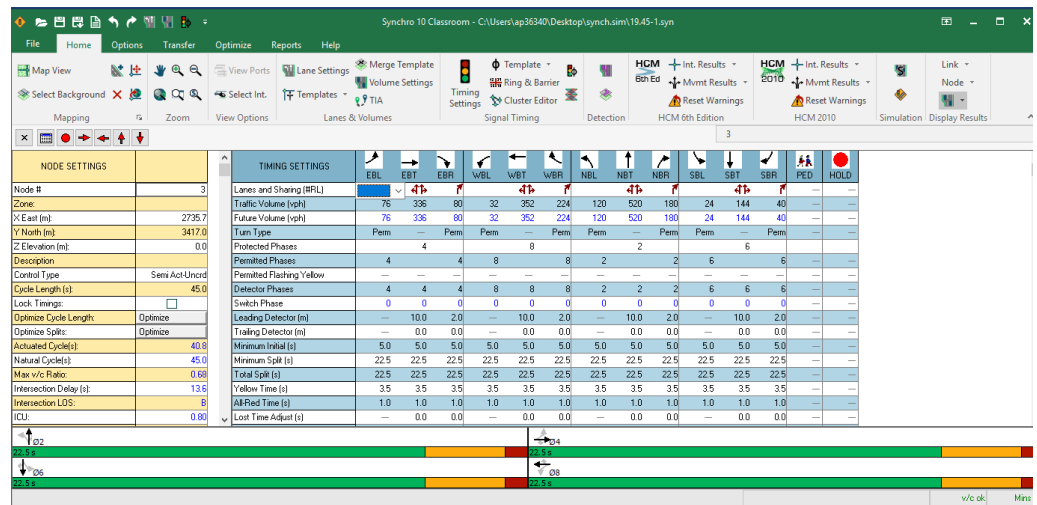
Figure 7. Screenshot of the Synchro interface for the TWC pattern.

We compare the three patterns for 60- and 80-s cycle lengths according to the performance measures D, PC, and DS in Sections 6.1, 6.2 and 6.3, respectively.

6.1. Comparison Based on the Delay Time

In this section, we compare the vehicle and pedestrian delays for signal patterns, TWC, LTI, and EPP. We first analyze the 80-s cycle length case. Figures 8 and 9 present the vehicle and pedestrian delay, respectively.
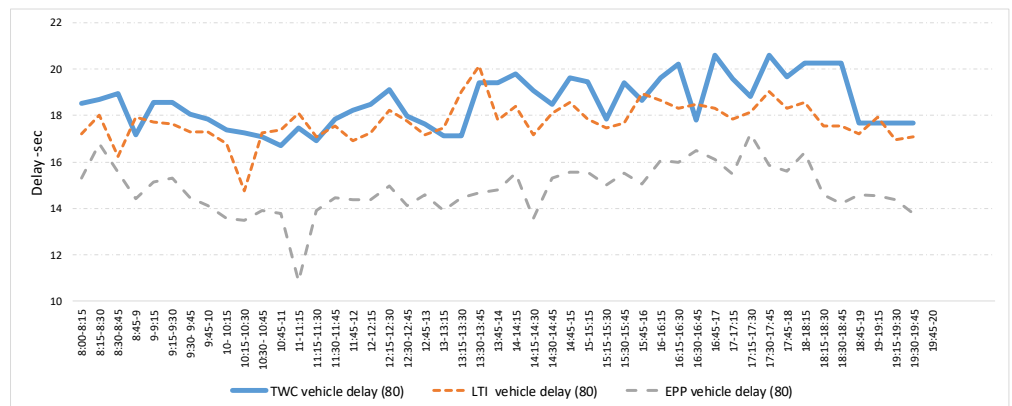

Figure 8. d^{veh-p} for 80-s cycle length, with $p \in \{TWC, LTI, EPP\}$.

Figure 8 presents the average vehicle delay for different signal patterns for each study period, d^{veh-p} for $p \in \{TWC, LTI, EPP\}$, during the day as returned by Synchro. We observe that EPP has the minimum vehicular delay during the day. This is due to the fact that, differently from the other patterns, the EPP vehicle green interval does not overlap with the pedestrian walk interval, while the cycle length is fixed for all patterns.
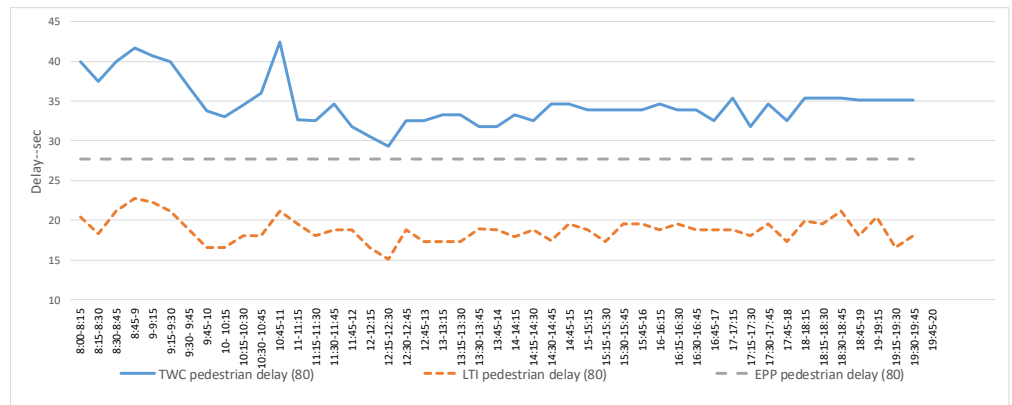
Figure 9. d^{ped-p} for 80-s cycle length, with $p \in \{TWC, LTI, EPP\}$.

Figure 9 depicts the average pedestrian delay of different patterns for each study period, d^{ped-p} for $p \in \{TWC, LTI, EPP\}$, computed according to Equations (21)–(23) in Section 4.1. According to this figure, the LTI pattern presents a minimum average pedestrian delay during the day.

Figure 10 shows the values of the weighted intersection delay D^p for $p \in \{TWC, LTI, EPP\}$ during the day as computed by Equation (3), and reflects the average waiting time of each user at the intersection. We observe that LTI is the overall best performing pattern, with an average delay of 18.17 s/user, followed by EPP. TWC is the least performing pattern in terms of D^p. It is worth noting that this is in contrast with what is reported in [9–11], where a greater delay for the EPP in comparison with the TWC is expected when pedestrian demand is low (such as 10:15, 14:15, and 19:00 in our case study). This discordance is due to the fact that this study modifies the pedestrian delay model by taking into account the detour delay and the conflict delay (Section 4.1). Figure 10 leads us to choose a combination of EPP and LTI as a hybrid pattern with the minimum delay for the day of study.
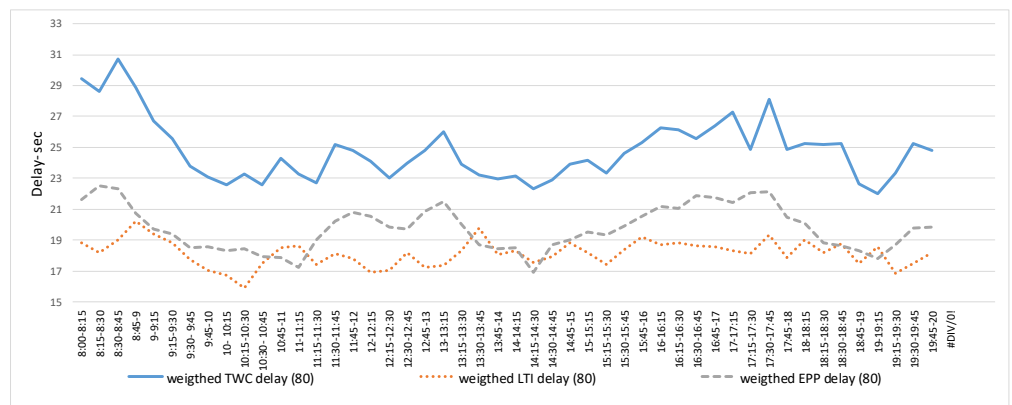

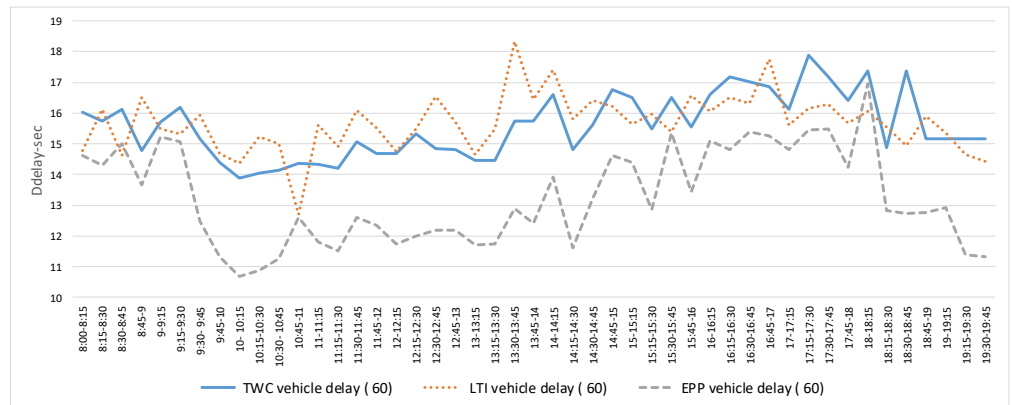**Figure 10.** D^p for 80-s cycle length, with $p \in \{TWC, LTI, EPP\}$.

According to the definition of the hybrid pattern in Section 3, this combination of LTI and EPP is called $H^D 80$ (hybrid delay pattern for 80-s cycle length) in our study, and it performs the traffic signal with 87.50% of LTI and 12.50% of EPP for the day of study.

Table 4 reports the delay improvement for the day of study when comparing the hybrid delay with the best performing single pattern. The table reports the pattern in the first column, and the weighted intersection delay the second column. We observe a 0.49% improvement for $H^D 80$ as compared to LTI, which is the best performing pattern.

**Table 4.** Hybrid improvement in comparison with the best performing pattern.

Pattern	*D* (s/User)
LTI	18.17
$H^D 80$	18.08
Improvement	0.49%

We repeated all the computations for the scenario with a fixed cycle length of 60 s. Figures 11 and 12 present the vehicle and pedestrian delays during the day for this scenario.

Figure 11. d^{veh-p} for 60-s cycle length, with $p \in \{TWC, LTI, EPP\}$.

Figure 11 reports the comparison of d^{veh-p} for $p \in \{TWC, LTI, EPP\}$. We observe that EPP is the best performing pattern in terms of vehicle delay time. We also observe that the maximum vehicle delay for EPP is reached at the vehicle peak hour volume.
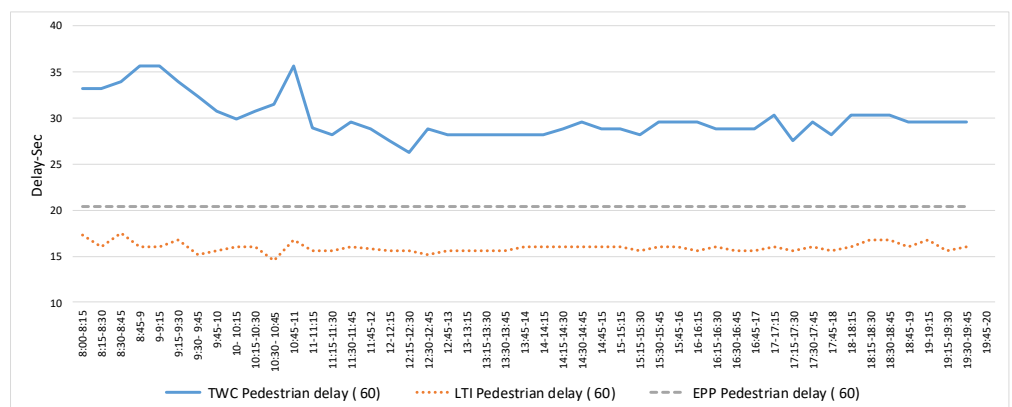
Figure 12. d^{ped-p} for 60-s cycle length, with $p \in \{TWC, LTI, EPP\}$.

Figure 12 reports a comparison of the pedestrian delay times for different patterns and for the 60-s cycle length. It shows that LTI has the smallest pedestrian delay during the day. This is due to the fact that the pedestrian green interval for the LTI is larger than that for the EPP.

Figure 13 presents the average weighted delay time during the day for the 60-s cycle length. We see that there is close competition between the EPP and LTI delay charts. This is in contrast with what reported in [19], where LTI was assessed superior to EPP.
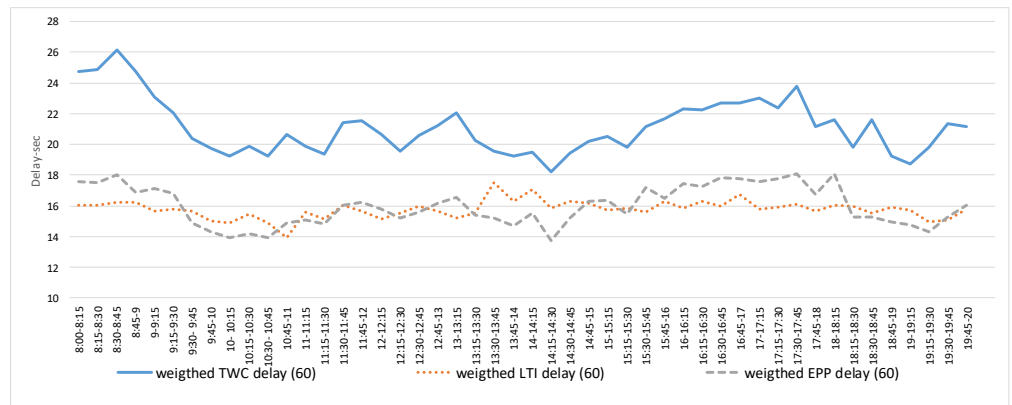
Figure 13. D^p with 60-s cycle length, with $p \in \{TWC, LTI, EPP\}$.

In the case of the 60-second cycle length, the hybrid delay 60 ($H^D 60$) has a portion consisting of 47.90% of EPP and 52.10% of LTI for the day of study. Table 5 compares the $H^D 60$ and the pattern with minimum delay. The first column presents the pattern, and the second one shows the average weighted delay.

Table 5. Hybrid improvement in comparison with the best performing pattern.

Pattern	D (s/User)
LTI	15.78
$H^D 60$	15.39
Improvement	2.47%

Table 5 reports the exact information of Table 4, but for a cycle length of 60 seconds and shows a 2.47% improvement in the intersection's delay when we run the $H^D 60$ as a pattern for the day of study. The $H^D 60$ reduces the delay for each user by 2.47% on our day of study.

To summarize, the results in this section show that the EPP and LTI patterns perform best in terms of vehicle and pedestrian delay, respectively. LTI is the best performing single pattern according to the weighted delay time. Furthermore, we have seen that the hybrid patterns $H^D(80)$ and $H^D(60)$ can potentially be improved over LTI.

6.2. Comparison Based on Potential Conflicts

Section 2.2.2 of this study investigates the performance indicators related to intersection safety. Potential user conflict represents a significant measure of unsafe situations for pedestrians and vehicles at the intersection. We compare the *PC* of patterns with 60- and 80-s cycle lengths. Figures 14 and 15 present pc^{v2v} and pc^{v2p} when the cycle length is 80 s for the case study intersection.

Figure 14 shows pc^{v2v} during the day. According to Equations (16)–(18), pc^{v2v} is related to the effective turning time. Therefore, it is similar for all three patterns since it is based on vehicle flow for every hour of study, and is not related to the cycle length or signal pattern.
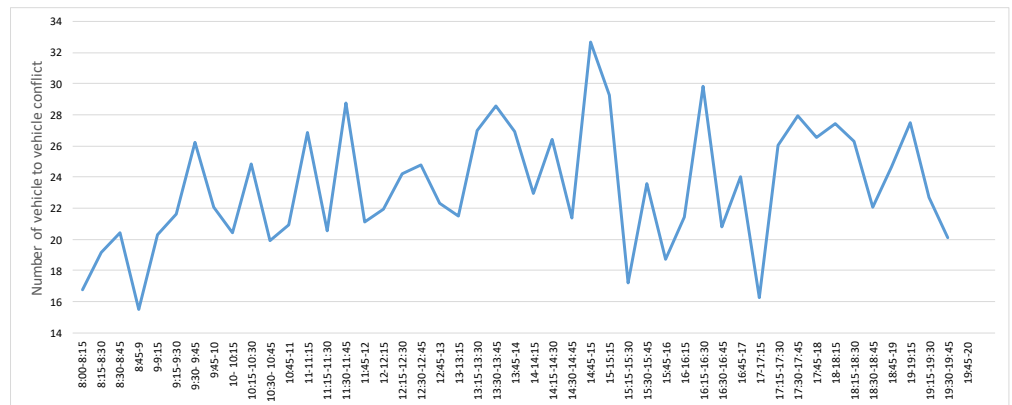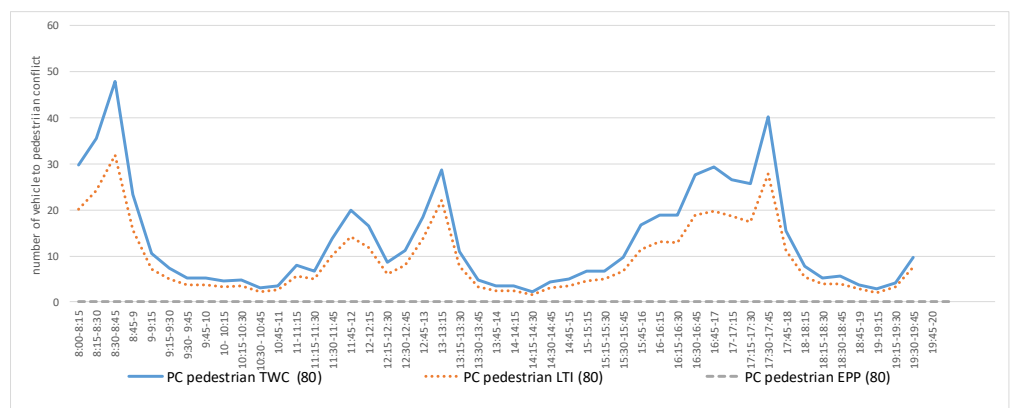
Figure 14. pc^{v2v} during the day.

Figure 15. pc^{v2p-p} for 80-s cycle length, with $p \in \{TWC, LTI, EPP\}$.

Figure 15 compares pc^{v2p-p} values during the day for $p \in \{TWC, LTI, EPP\}$ when Equations (28) and (29) are applied to compute pc^{v2p-p}. Since it is assumed that the pedestrian always respects traffic signal rules, pc^{v2p} for EPP is considered zero. In comparison with TWC, LTI in Figure 15 shows fewer pedestrian conflicts, specifically at peak pedestrian periods.

Figure 16 compares the total number of potential conflicts at the intersection for $p \in \{TWC, LTI, EPP\}$ based on Equations (30)–(32), for each study period and shows that EPP has the minimum number of conflicts during the day. The figure shows three periods of the day in which LTI and EPP have the same number of potential conflicts; these pedestrian volume values for these periods are in the order of less than 250 pedestrians per 15 min.
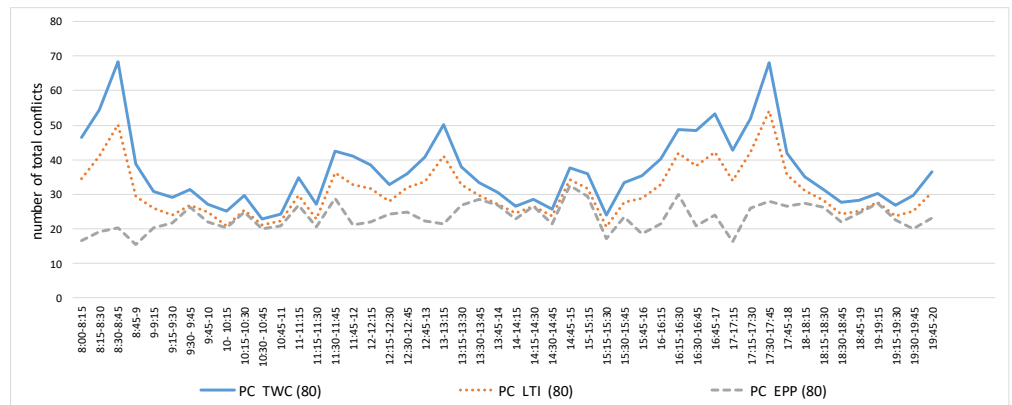
Figure 16. PC^p for 80-s cycle length, with $p \in \{TWC, LTI, EPP\}$.

Table 6 compares the best performing pattern in terms of the numbers of potential conflicts (PC), with the hybrid pattern $H^{PC}80$. $H^{PC}80$ has no improvement since EPP is the only pattern composing the $H^{PC}80$. We performed the same computational experiment for a 60-s cycle length, and the results are discussed next.

Table 6. Hybrid improvement in comparison with the best performing pattern.

Pattern	PC (Users with Conflict/15 min)
EPP	23.09
$H^{PC}80$	23.09
Improvement	0%

Similar to Figure 15, Figure 17 compares pc^{v2p} for $p \in \{TWC, LTI, EPP\}$, but with a 60-s cycle length. In both the 60-s cycle length pc^{v2v} and pc^{v2p}, the EPP presents the minimum potential conflict during the day.
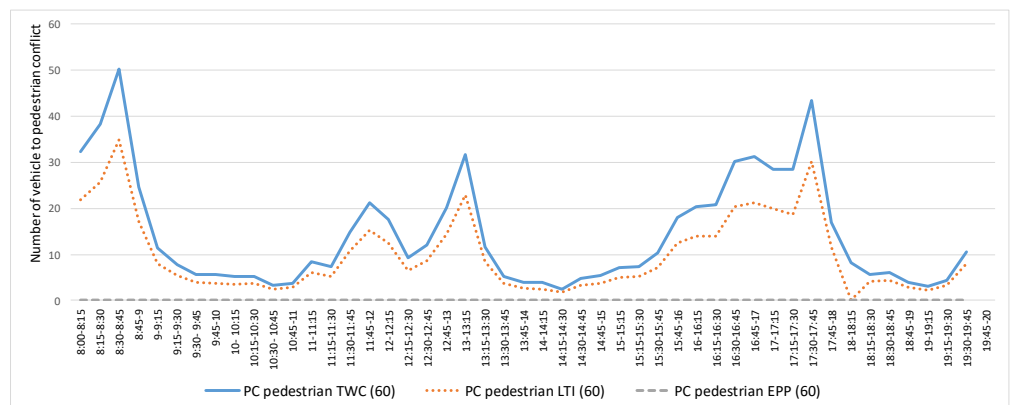

Figure 17. pc^{v2p-p} for 60-s cycle length, with $p \in \{TWC, LTI, EPP\}$.

Figure 18 presents the same information as Figure 16, but with a 60-s cycle length, and reports the EPP as the minimum number of potential conflicts for our study period. Table 7 presents the same information as Table 6, but for a 60-s cycle length setting.
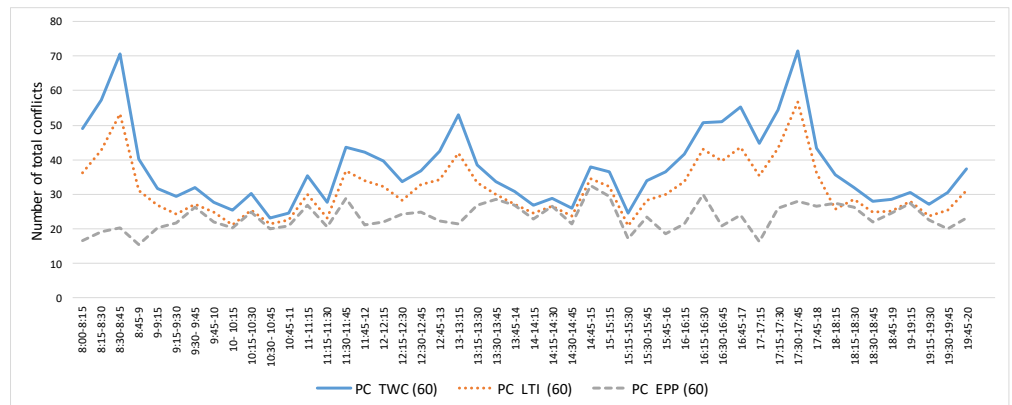
Figure 18. PC^p for 60-s cycle length, with $p \in \{TWC, LTI, EPP\}$.

Table 7. Hybrid improvement in comparison with the best performing pattern.

Pattern	PC (Users with Conflict/15 min)
EPP	23.09
$H^{PC}60$	23.09
Improvement	0%

Table 7 reports the same information as Table 6 when the cycle length is 60 s. As for the previous case, also $H^{PC}60$ does not improve over the best performing EPP pattern. We observe that H^{PC} reports the same amount of conflicts for 60- and 80-s cycle lengths, since for the EPP pattern, $pc^{v2p} = 0$ and PC^{EPP} score the same as pc^{v2v} for both cycle lengths.

6.3. Comparison Based on the Delay and Safety Index

Section 4.3 of this study investigates *DS* (Delay and Safety index) as a combination of delays and a potential number of conflicts related to the user volume at the intersection.

In this section, we compare the DS^{veh-p} and DS^{ped-p} computed according to Equations (34) and (35), respectively. The first experiment compares *DS* for different patterns with an 80-s cycle lengths. Figure 19 compares DS^{veh-p} for $p \in \{TWC, LTI, EPP\}$, with an 80-s cycle length. It shows that the EPP pattern provides the most acceptable *DS* during the day, when only vehicles are considered in our study.

Figure 20 presents a comparison of DS^{ped-p} for $p \in \{TWC, LTI, EPP\}$ for the day of study. It reports LTI as the best performing pattern in terms of DS^{ped}.

Figure 19. DS^{veh-p} for 80-s cycle length, with $p \in \{TWC, LTI, EPP\}$.
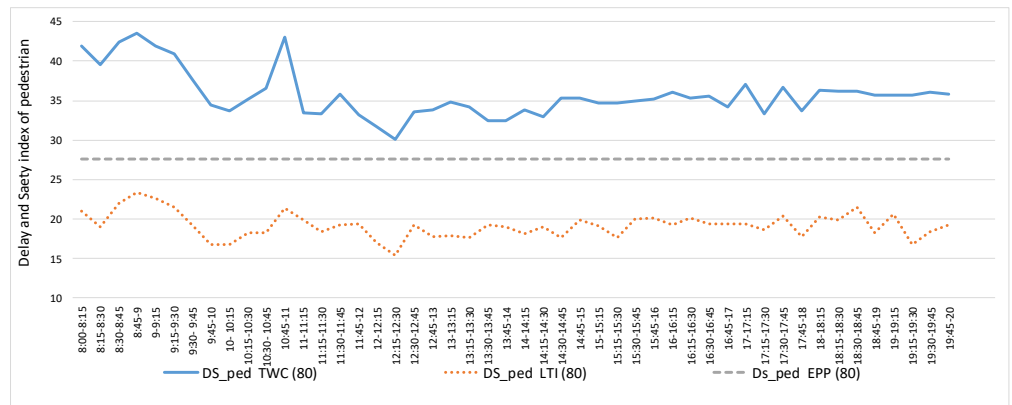
Figure 20. DS^{ped-p} for 80-s cycle length, with $p \in \{TWC, LTI, EPP\}$.

Figure 21 presents a comparison of DS for $p \in \{TWC, LTI, EPP\}$ for the study day when both user delay and conflict are taken into account to calculate DS, according to Equation (33). Figure 21 proposes the hybrid pattern as a more efficient pattern during the day of study. The hybrid DS (80) ($H^{DS}80$) leads mainly to the LTI pattern (87.50%), and occasionally to EPP (12.50%) during the day.
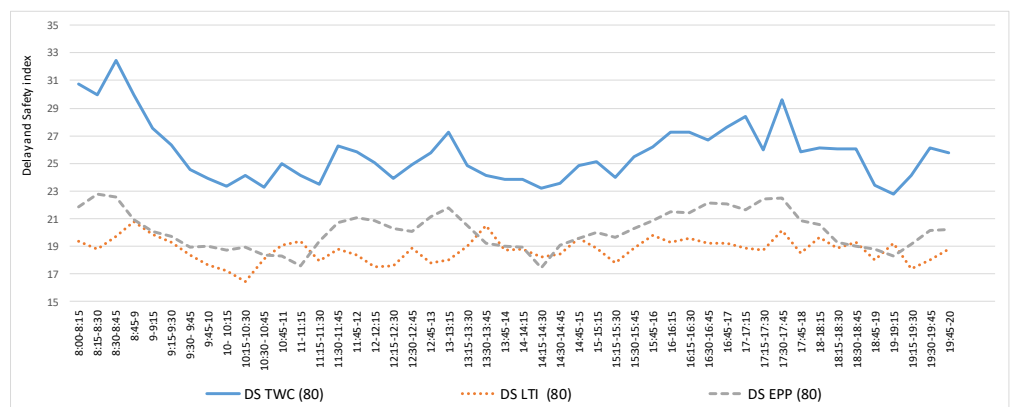

Figure 21. DS^{p} comparison for 80-s cycle length, with $p \in \{TWC, LTI, EPP\}$.

Table 8 presents a comparison of $H^{DS}80$ with the best performing pattern, where the first column shows the pattern and the second column presents the average DS for that pattern for the study day. The $H^{DS}80$ reduces the average Delay and Safety index of each user for the study day by 0.64%, marking an improvement of the level of service and of safety for each user.

Table 8. Hybrid improvement in comparison with the best performing pattern.

Pattern	DS (s/User)
LTI	18.77
$H^{DS}80$	18.65
Improvement	0.64%

In the next section, we repeat the computation of DS^{veh-p} and DS^{ped-p} with a 60-s cycle length. Figure 22 compares DS^{veh-p} for different patterns and presents the EPP as the pattern with the minimum DS, but not for all periods of study. In this investigation, the hybrid pattern is presented as a combination of two patterns; however, the figure mainly is mainly comprised of the EPP.
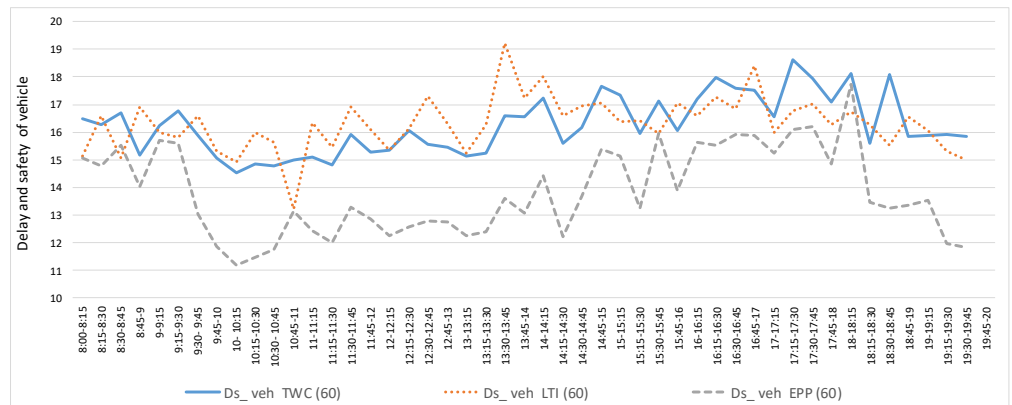
Figure 22. DS^{veh-p} for 60-s cycle length, with $p \in \{TWC, LTI, EPP\}$.

Figure 23 presents a comparison of DS^{ped-p} for $p \in \{TWC, LTI, EPP\}$ during the day of study. Here, LTI is the more efficient pattern since both pedestrian delay and conflict are included in our investigation.
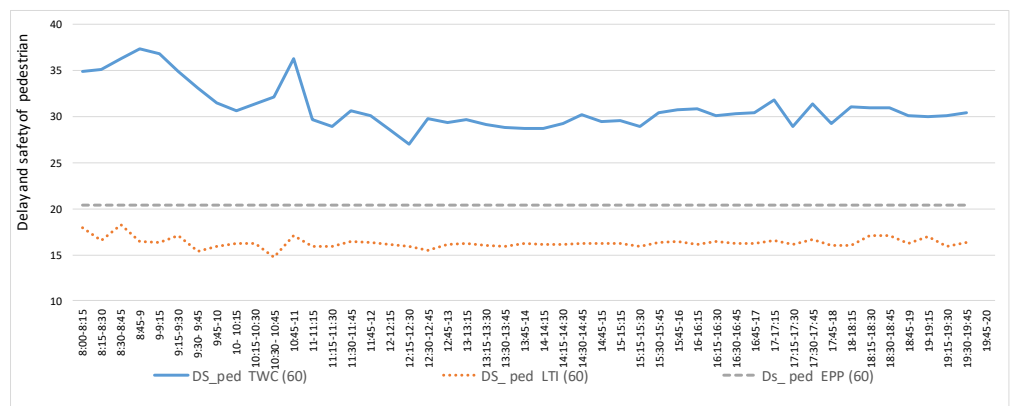
Figure 23. DS^{ped-p} for 60-s cycle length, with $p \in \{TWC, LTI, EPP\}$.

Figure 24 compares the intersection DS for all three study patterns. From this comparison, we get the hybrid $DS60$ ($H^{DS}60$), which does not show any dominant pattern, with $H^{DS}60$ constantly fluctuating between LTI and EPP during the day. In fact, on the day of study the composition of H^D60 breaks down to 50.00% EPP and 50.00% LTI. Table 9 contains the same information as Table 7, but with a 60-s cycle length setting.

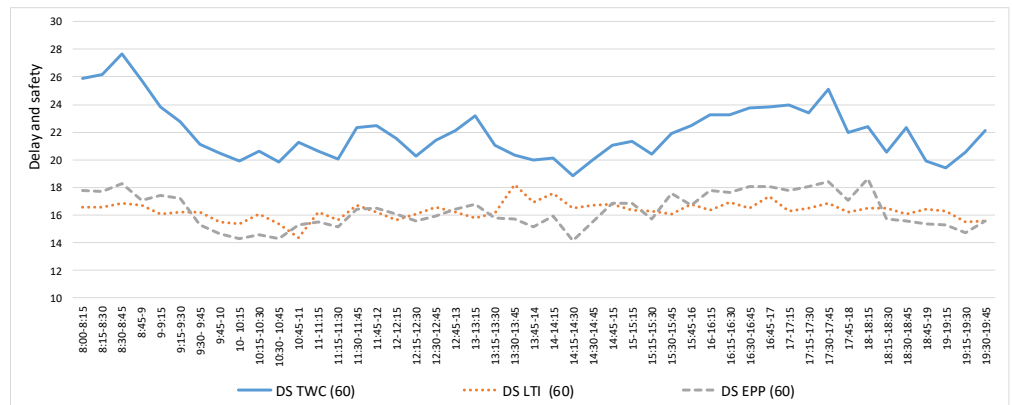**Figure 24.** DS^p for 60-s cycle length, with $p \in \{TWC, LTI, EPP\}$.

Table 9. Hybrid improvement in comparison with the best performing pattern.

Pattern	DS (s/User)
LTI	16.42
$H^{DS}60$	15.85
Improvement	3.47%

Table 9 presents a comparison of $H^{DS}60$ and the best performing pattern, and shows a 3.47% improvement of DS when we choose $H^{DS}60$ over the LTI as the pattern with the minimum DS. It improves the average Delay and Safety index for each user by 3.47%.

The study reports the EPP and LTI as the single patterns with the minimum DS for the cycle length of 80 and 60, respectively, while the hybrid pattern shows slight improvement over both fixed cycle lengths.

6.4. Analysis of Performance Measures Related to Hybrid Patterns

In the last section, we obtained the hybrid pattern for each performance measure (D, PC, and DS). This section compares the performance of hybrid patterns when considering 60 and 80-s cycle lengths. Results are reported in Tables 10 and 11, which compare the performance of the hybrid patterns. In each case, the first and second columns identify the considered pattern and its unit of measure. The third, fourth and fifth columns report D, PC, and DS averages over the operating day for each hybrid pattern.

Table 10. Comparison of 80-s cycle length hybrid patterns in terms of delay, conflict and DS.

Pattern	Unit of Measure	$H^D\,80$	$H^{PC}\,80$	$H^{DS}\,80$
D	s/user	18.08	19.83	18.08
PC	user with conflict/15 min	28.98	23.09	28.96
DS	s/user	18.90	20.22	18.65

From Table 10, we infer that H^D80 is the best performing pattern in terms of delay time. This result is not surprising considering that the patterns composing H^D80 have been chosen to minimize the delay time. However, we also observe that H^D80 is the worst-performing algorithm in terms of potential conflict. In other terms, patterns minimizing the delay time generally expose users to higher risks of conflict. The situation is inverted for $H^{PC}80$ as the best performing pattern in potential conflict but the worst pattern in terms of delay time. Again, potential conflict and delay time are conflicting objectives and minimizing one results in a deteriorated performance for the other. In this sense, Table 10 suggests that $H^{DS}80$ provides an excellent compromise in terms of delay time and potential conflicts. It scores a delay time of 18.08 s, which is similar to a delay time of H^D80, and

the number of potential conflicts of 28.96, against 23.09 of $H^{PC}80$. In the second case, we compare the performance of each 60-s cycle length hybrid pattern in Table 11.

Table 11. Comparison of 60-s cycle length hybrid patterns in terms of delay, conflict and DS.

Pattern	Unit of Measure	H^D 60	H^{PC} 60	H^{DS} 60
D	s/user	15.39	16.07	15.41
PC	user with conflict/15 min	29.91	23.09	29.31
DS	s/user	15.98	16.41	15.85

Similar to the previous case, Table 11 shows that the H^D60 pattern with a minimum delay and H^{PC} 60 pattern with a minimum conflict. Table 11 also suggests that $H^{DS}60$ provides an excellent compromise in terms of delay time and potential conflicts. It scores a delay time of 15.41 s, against the 15.39 s of H^D60, and the number of potential conflicts of 29.31 against 23.09 of $H^{PC}60$.

From Tables 10 and 11 it can be seen that the 60-s cycle length improves for all three performance indicators versus the 80-s cycle length case, suggesting that the current configuration (80 s) is sub-optimal.

Table 12 presents improvements of the hypothetical hybrid pattern obtained by dynamically adapting the signal pattern to real-time data, over the best performing single pattern measured by the three performance indicators (D, PC, DS). Results show that the hybrid pattern H^D was able to improve the D by 0.49% and 2.47%, for the 60 and 80-s cycle lengths, respectively. Similarly, H^{DS} improved the DS by 0.58% and 3.47%, for the 60 and 80 cycle lengths, respectively. However, H^{PC} did not improve versus the best performing single pattern. The improvements of H^D and H^{DS} are explained by the fact that both these hybrid patterns are composed of a combination of LTI and EPP. On the contrary, H^{PC} is entirely composed of EPP, and thus there is no advantage in adopting a hybrid pattern. Further analyzing Table 12, we also observe that hybrid patterns provide greater improvements for the 60-s cycle length. We argue that this is due to the fact that the best performing single pattern constitutes a smaller portion of the hybrid patterns for the 60-s cycle length relative to the 80 s case. For example, the best performing single-pattern makes up 50.00% of the hybrid $H^{DS}60$, whereas for the hybrid $H^{DS}80$, this portion becomes 87.5%. A more detailed discussion on this can be found in the next section, where we propose several sensitivity analyses.

Table 12. Improvement of hybrid patterns in comparison with best performing patterns.

Cycle Length	Percentage of Improvement		
	H^D	H^{PC}	H^{DS}
80	0.49	0	0.58
60	2.47	0	3.47

6.5. Sensitivity Analyses

To enrich our computational study, in this section, we perform several sensitivity analyses on the variation of two important elements: (1) the passenger occupancy rate (the average number of passengers carried by vehicles), and (2) the relative weight of the potential vehicle-to-pedestrian conflict (pc^{v2p}) relative to the potential vehicle-to-vehicle conflict (pc^{v2v}). Both these analyses require parameterizing some of the equations involved in the performance indicator evaluations, together with performing extensive computational experiments. Given that the previous section showed that the 60-s cycle length case consistently outperformed the 80-s case, we only focus on the 60-s case in this section.

The first analysis focuses on the impact of the passenger occupancy rate (we denote it α) on the performance of the hybrid patterns. Variations of α will require parametrizing the weights in the weighted averages in Equations (3) and (33). These equations are modified by substituting V^{veh} by αV^{veh} as follows:

$$D^p = \frac{d^{veh-p}\alpha V^{veh} + d^{ped-p}V^{ped}}{\alpha V^{veh} + V^{ped}} \quad \alpha \geq 1 \ p \in \{TWC, LTI, EPP\} \quad (s/user) \qquad (36)$$

and

$$DS^p = \frac{DS^{veh-p}\,\alpha V^{veh} + DS^{ped-p}\,V^{ped}}{\alpha V^{veh} + V^{ped}} \quad \alpha \geq 1 \ p \in \{TWC, LTI, EPP\} \quad (s/user) \qquad (37)$$

Note that α does not affect PC measure, and therefore, PC is not considered in the proposed analysis.

The European Environment Agency and The US Office of Energy Efficiency and Renewable Energy have reported that the average passenger occupancy rate is approximately 1.45 [38] and 1.59 [39] per vehicle (including the driver), respectively. Thus, in our study, we let α vary in $\{1, 1.2, 1.4, 1.6, 1.8, 2\}$. For each of these values, we recompute the measures D and DS and determine the best performing single pattern and the hybrid pattern.

Figure 25 shows the composition of the hybrid pattern in terms of proportions of the basic patterns when optimizing the delay time. We observe that TWC is never chosen, and the hybrid pattern is composed of varying portions of LTI and EPP. In particular, the portion of EPP increases from 45.84% for $\alpha = 1.2$ to 68.75% for $\alpha = 2$. This might be due to the fact that EPP generally provides better performance in terms of vehicle delays (see Figure 11).
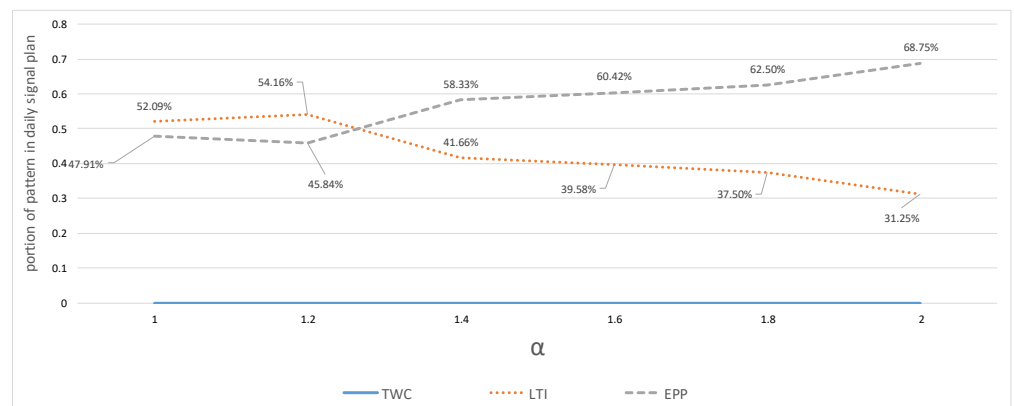

Figure 25. Portion of signal pattern in $H^D 60$ by varying values of α.

To understand how the improvements of the hybrid pattern change with α, we compared the delay time of $H^D 60$ with the best performing single pattern in Table 13, where the first column refers to α and the following columns present D for the $H^D 60$, the best performing pattern for each value of α and the improvement percentage, while we choose $H^D 60$ over the best performing pattern, respectively. We observe that the improvements range from 2.12% to 3.23%. We cannot, however, identify a monotonic relation between improvements and values of α.

Table 13. Comparison of D for $H^d 60$ and the best performing pattern.

α	D for $H^d 60$	D for the Best Performing Pattern	Percentage of Improvement
1	15.39	15.78	2.47
1.2	15.26	15.77	3.23
1.4	15.08	15.55	3.02
1.6	14.95	15.36	2.66
1.8	14.84	15.20	2.36
2	14.74	15.06	2.12

We repeat the methodology of the previous experiment to study the impact of α on DS. Figure 26 shows the composition of the hybrid pattern in terms of the proportion of

the basic patterns when optimizing *DS*. Similar to the Delay Time case, we observe that TWC is never chosen in the hybrid pattern. Furthermore, following a similar pattern as in the previous experiment, the portion of EPP in the hybrid pattern increases with α, and in particular, ranges from 50.00% to 77.08%. This tendency might still be due to the fact that EPP performed particularly well in terms of Vehicle Delay Time.
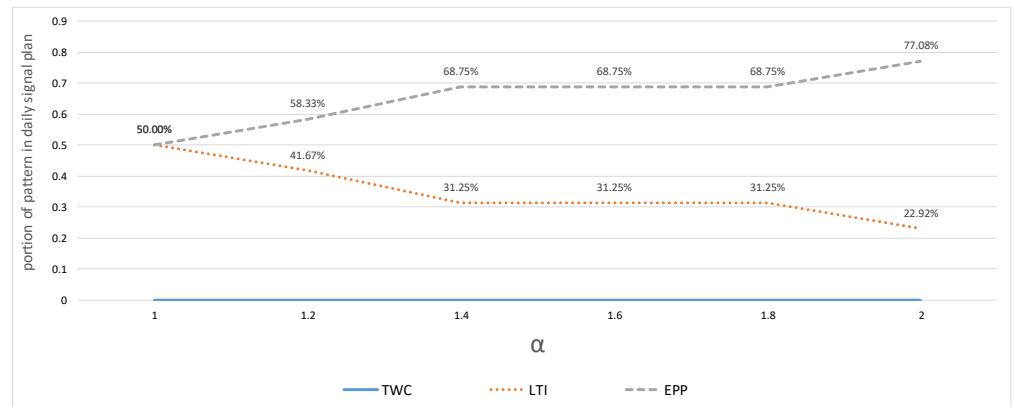

Figure 26. Portion of signal pattern in $H^{DS}60$ by varying values of α.

Table 14 shows improvements of the hybrid pattern $H^{DS}60$ relative to the best performing single pattern. The meaning of each column is similar to what is provided in Table 13, but in Table 14, instead of D, DS is investigated. We observe that the improvements of $H^{DS}60$ range from 1.07% to 3.47%. Differently from the previous case, here, we identify a monotonous relation between the improvements and α. In particular, we observe that by increasing the value of α, the efficiency of the hybrid pattern over the best performing pattern decreases. This is due to the fact that when α increases, the performance of the EPP pattern in terms of DS also increases, and consequently, the portion of EPP composing the hybrid $H^{DS}60$ also increases by up to 77.08%. We also observe that LTI still outperforms EPP for time periods with high pedestrian volumes.

Table 14. Comparison of DS for $H^{DS}60$ and the best performing pattern.

α	DS of $H^{DS}60$	DS of the Best Performing Pattern	Percentage of Improvement
1	15.85	16.42	3.47
1.2	17.53	17.96	2.39
1.4	19.42	19.75	1.67
1.6	21.41	21.72	1.42
1.8	23.55	23.81	1.09
2	25.73	26.01	1.07

The second sensitivity analysis focuses on the impact of changing the relative weight of pc^{v2p} relative to pc^{v2v}. This mostly requires parametrizing Equation (27) by substituting pc^{v2p-p} with σpc^{v2p-p}, where σ is a suitable weighting factor:

$$PC^p = pc^{v2v} + \sigma pc^{v2p-p} \quad sigma \geq 1 \quad (user\ with\ conflict\ /time\ interval) \quad (38)$$

We observe that changes in σ do not have any impact on the Delay Time, which is consequently excluded from further analysis. Concerning the Delay and Safety index, we need to modify Equation (35) as follows:

$$DS^{ped-p} = d^{ped-p}\left(1 + \frac{\sigma pc^{v2p-p}}{V^{ped}}\right) \quad sigma \geq 1 \quad (s/user) \quad (39)$$

To the best of our knowledge, the literature does not provide a methodology to assign suitable values to σ or to estimate the impacts of a given value in terms of fatalities, injuries, etc. [40]. However, when comparing the fatality, major injury and minor injury counts due to a given value of pc^{v2v}, Zhang et al. (2003) [32] estimate that the corresponding count for the same value of pc^{v2p-p} is about 12, 6 and 1.7 times higher, respectively. In practice, traffic agencies set the value of σ for pc^{v2p-p} by rules of thumb [40]. In this study, we let σ vary in $\{1, 2, 3, 4, 5, 6\}$.

As shown in Figure 17, EPP scores a value of $pc^{v2p} = 0$. Furthermore, $H^{PC}60$ is completely composed of EPP, and therefore, the PC will not change, even by varying σ; as well, EPP will remain the best performing pattern in terms of *PC*. Therefore, we will now concentrate on studying the performance of $H^{DS}60$.

Figure 27 presents the composition of the hybrid pattern in terms of proportion of basic patterns when optimizing the *DS*. We observe that, as in all previous experiments, TWC is never chosen as part of the hybrid pattern. This pattern is only composed of LTI and EPP, with EPP increasing from 50.00% to 66.66%. This increase is due to the fact that $pc^{v2p} = 0$ for EPP, and thus, increasing σ has no impact on EPP, while it deteriorates the performance of the other patterns.
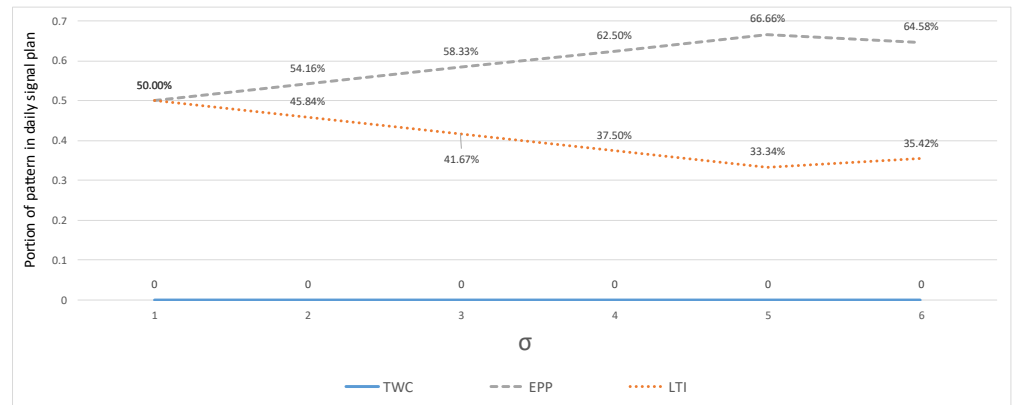

Figure 27. Portion of the signal pattern in $H^{DS}60$ by varying values of σ.

Table 15 presents the improvements seen in the hybrid patterns $H^{DS}60$ relative to the best performing single pattern when varying σ. The meaning of each column is similar to what is provided in Table 14, but, instead of α, we now vary the parameter σ in the first column. We observe that improvements range from 0.73% to 3.41%. We also observe the existence of a monotonic relation between σ and the improvements. Specifically, the improvements decrease with as σ increases. This is probably due to the fact that EPP constitutes a larger portion of the hybrid $H^{DS}60$ when σ increases. In fact, larger values of σ imply a larger penalization of pedestrian-to-vehicle conflicts, and EPP performs particularly well in terms of this performance measure. We note that LTI is still competitive in time periods with low pedestrian volumes.

Table 15. Comparison of *DS* for $H^{DS}60$ and the best performing pattern.

σ	*DS* of $H^{DS}60$	*DS* of the Best Performing Pattern	Percentage of Improvement
1	15.85	16.41	3.41
2	15.95	16.41	2.80
3	16.05	16.41	2.19
4	16.15	16.41	1.58
5	16.22	16.41	1.15
6	16.29	16.41	0.73

6.6. Limitations and Recommendations

This research is naturally subject to limitations that need to be investigated. Below are recommendations for future research paths. The result of our study only applies to one specific intersection on one specific day. This study should be performed on other intersections and for different time periods to account for a variety of user flow rates as this should provide reliable results regarding how traffic signal performance indicators are impacted by dynamically changing signal patterns.

In this study, because of the limitations of the software used, the effects of signal patterns on the intersection's performance indicators were investigated using only a fixed cycle length. Therefore, it is recommended to investigate the effect of changing or optimizing both the cycle length and the signal pattern on the performance indicators.

In our study we made the hypothesis that the Peel-Notre-Dame intersection is isolated. In reality some interaction with close-by intersections may exist. It is then recommended to investigate the coordination between intersections.

According to general observations, 20.00% of pedestrians cross the intersection during the flashing or red intervals. However, in this study, we considered that all pedestrians were crossing during the green interval. Therefore, further research is needed to assess the impact of pedestrian behavior on the performance of traffic signal patterns.

Finally, it is recommended that future studies investigate how users deal with the signal pattern changing dynamically as this may affect users' behavior and, in turn, the effectiveness of dynamically changing the signal patterns.

7. Conclusions

This study investigates how dynamically changing the traffic signal pattern configuration allows to better accommodate traffic flow variation throughout the day. More specifically, this research aims to determine whether an optimized hybrid pattern can decrease the travel time and increase safety at the intersection for both vehicles and pedestrians.

To investigate the impact of a hybrid pattern on traffic flow and safety performance, methods used to measure the delay (D), conflict situations (PC), and Delay and Safety index (DS) were adapted to include both vehicles and pedestrians for different signal patterns (TWC, EPP, and LTI). The methods were applied to the Notre-Dame-and-Peel intersection in Montreal. The traffic data of the intersection was collected and simulated. Video data were collected on Wednesday, 8 October 2018, from 8 a.m. to 8 p.m. Then, traffic data was simulated on Synchro. Finally, performance indicators (D, PC, DS) were computed based on the real-time traffic data and Synchro outputs.

The case study results show the effect of each signal pattern considered by the study on the performance indicators. EPP is shown to be the best performing pattern, for a fixed cycle length of 80 and 60 s, regarding PC, while LTI is shown to be the best performing single pattern regarding D and DS. A dynamic hybrid pattern is developed by combining LTI and EPP when considering DS or D as performance indicators. However, for PC, the dynamic hybrid pattern consists of EPP only as it is the best performing pattern.

Among the three hybrid patterns formulated in the study, H^{DS} was the best performing one, improving the average intersection DS. A comparison of the $H^{DS}80$ and $H^{DS}60$ with the best performing non-hybrid pattern shows a 0.58% and 3.47% improvement in DS, respectively. Therefore, the hybrid pattern has a favorable but limited impact on the quality of travel at the intersection for the one day of data used in this study. However, further research based on additional observations made on different days is needed to verify whether the hybrid pattern significantly improves the quality of travel.

Author Contributions: Writing—review & editing, F.M., F.E. and L.P. All authors have read and agreed to the published version of the manuscript.

Conflicts of Interest: The authors declare that there is no conflict of interest.

References

1. Signalized Intersections. In *Highway Capacity Manual—A Guide for Multimodal Mobility Analysis*, 6th ed.; Transportation Research Board: Washington, DC, USA, 2016.
2. Stevanovic, A.; Stevanovic, J.; So, J.; Ostojic, M. Multi-criteria optimization of traffic signals: Mobility, safety, and environment. *Transp. Res. Part Emerg. Technol.* **2015**, *55*, 46–68. [CrossRef]
3. Jia, H.; Lin, Y.; Luo, Q.; Li, Y.; Miao, H. Multi-objective optimization of urban road intersection signal timing based on particle swarm optimization algorithm. *Adv. Mech. Eng.* **2019**, *11*, 1687814019842498. [CrossRef]
4. Builenko, V.; Pakhomova, A.; Pakhomov, S. Optimization of the method for collecting source data to calculate the length of the traffic light control cycle. *Transp. Res. Procedia* **2018**, *36*, 90–94. [CrossRef]
5. Chen, X.; Osorio, C.; Santos, B.F. Simulation-based travel time reliable signal control. *Transp. Sci.* **2019**, *53*, 523–544. [CrossRef]
6. Li, Z.; Shahidehpour, M.; Bahramirad, S.; Khodaei, A. Optimizing Traffic Signal Settings in Smart Cities. *IEEE Trans. Smart Grid* **2017**, *8*, 2382–2393. [CrossRef]
7. Li, X.; Sun, J.Q. Multi-objective optimal predictive control of signals in urban traffic network. *J. Intell. Transp. Syst. Technol. Planning Oper.* **2019**, *23*, 370–388. [CrossRef]
8. Wong, C.K.; Wong, S.C. Lane-based optimization of signal timings for isolated junctions. *Transp. Res. Part Methodol.* **2003**, *37*, 63–84. [CrossRef]
9. Ishaque, M.M.; Noland, R.B. Trade-offs between vehicular and pedestrian traffic using micro-simulation methods. *Transp. Policy* **2007**, *14*, 124–138. [CrossRef]
10. Zhang, Y.; Su, R. Pedestrian Phase Pattern Investigation in a Traffic Light Scheduling Problem for Signalized Network. In Proceedings of the 2018 IEEE Conference on Control Technology and Applications, CCTA, Copenhagen, Denmark, 21–24 August 2018; pp. 608–613. [CrossRef]
11. Ma, W.; Liao, D.; Liu, Y.; Lo, H.K. Optimization of pedestrian phase patterns and signal timings for isolated intersection. *Transp. Res. Part Emerg. Technol.* **2015**, *58*, 502–514. [CrossRef]
12. Feng, Y.; Duives, D.; Daamen, W.; Hoogendoorn, S. Data collection methods for studying pedestrian behaviour: A systematic review. *Build. Environ.* **2021**, *187*, 107329. [CrossRef]
13. Alavi, H.; Charlton, J.; Newstead, S. Factors driving intersection pedestrian crash risk in concentrated urban environments. *J. Road Saf.* **2013**, *32*.
14. Torbic, D.J.; Harwood, D.W.; Bokenkroger, C.D.; Srinivasan, R.; Carter, D.; Zegeer, C.V.; Lyon, C. Pedestrian safety prediction methodology for urban signalized intersections. *Transp. Res. Rec.* **2010**, *2198*, 65–74. [CrossRef]
15. Sayed, T.; Zein, S. Traffic conflict standards for intersections. *Transp. Plan. Technol.* **1999**, *22*, 309–323. [CrossRef]
16. Li, X.; Yan, X.; Li, X.; Wang, J. Using cellular automata to investigate pedestrian conflicts with vehicles in crosswalk at signalized intersection. *Discret. Dyn. Nat. Soc.* **2012**. [CrossRef]
17. Frankish, C.J.; Green, L.W.; Ratner, P.A.; Chomik, T.; Larsen, C. Health Impact Assessment as a Tool for Health Promotion and Population Health. In *Technical Report 9*; World Health Organization: Geneva, Switzerland, 2003.
18. Urbanik, T.; Tanaka, A.; Lozner, B.; Lindstrom, E.; Lee, K.; Quayle, S.; Beaird, S.; Tsoi, S.; Ryus, P.; Gettman, D.; et al. *Signal Timing Manual*, 2nd ed.; Transportation Research Board: Washington, DC, USA, 2015. [CrossRef]
19. Furth, P.G.; Saeidi Razavi, R.M. Leading Through Intervals versus Leading Pedestrian Intervals: More Protection with Less Capacity Impact. *Transp. Res. Rec.* **2019**, *2673*, 152–164. [CrossRef]
20. Tom V. Mathew. Signalized Intersection Delay Models for Non lane-Based Heterogeneous Traffic at Signalized Intersections. *Transp. Syst. Eng.* **2014**, *136*, 1–18.
21. Li, J.; Rouphail, N.; Akcelik, R. Overflow delay estimation for a simple intersection with fully actuated signal control. *Transp. Res. Rec.* **1994**, *1457*, 73–81.
22. Wagner, P.; Gartner, N.H.; Lu, T.; Oertel, R. *Webster's Delay Formula–Revisited*; Transportation Research Board: Washington, DC, USA, 2013.
23. Roshandeh, A.M.; Li, Z.; Zhang, S.; Levinson, H.S.; Lu, X. Vehicle and pedestrian safety impacts of signal timing optimization in a dense urban street network. *J. Traffic Transp. Eng. (Eng. Ed.)* **2016**, *3*, 16–27. [CrossRef]
24. Hadiuzzaman.; Rahman, M.; Hasan, T.; Karim, A. Development of Delay Model for Non-Lane Based Traffic at Signalized Intersection. *Int. J. Civ. Eng. (IJCE)* **2014**, *3*, 67–82.
25. Ma, W.; Liu, Y.; Head, K.L. Optimization of pedestrian phase patterns at signalized intersections: A multi-objective approach. *J. Adv. Transp.* **2014**, *48*, 1138–1152. [CrossRef]
26. Yang, Z. Signal Timing Optimization Based on Minimizing Vehicle and Pedestrian Delay by Genetic Algorithm. Ph.D. Thesis, University of Illinois at Urbana-Champaign, Champaign, IL, USA, 2010.
27. Brow, G. Traffic conflicts for road user safety studies. *Can. J. Civ. Eng.* **2011**, *21*, 1–15. [CrossRef]
28. Lord, D. Analysis of pedestrian conflicts with left-turning traffic. *Transp. Res. Rec.* **1996**, *1538*, 61–67. [CrossRef]

29. Matsui, Y.; Takahashi, K.; Imaizumi, R.; Ando, K. Car-to-pedestrian contact situations in near-miss incidents and real-world accidents in japan. *Yasuhiro Matsui Kunio Takahashi Ryoko Imaizumi Kenichi Ando* **2012**, *66*, 37–39.

30. Majeed, R.; Ewadh, H. A Conflict Index to Assess Traffic Safety at Intersections. *IOP Conf. Ser. Mater. Sci. Eng.* **2019**, *584*, 12018. [CrossRef]

31. Chang, C.M.; Rodriguez, E.D. Vulnerable road user safety enhancements for transportation asset management center for transportation, environment, and community health final report. In *Technical Report*; Center for Transportation, Environment, and Community Health: Washington, DC, USA, 2019.

32. Zhang, L.; Prevedouros, P. Signalized intersection level of service incorporating safety risk. *Transp. Res. Rec.* **2003**, *1852*, 77–86. [CrossRef]

33. Li, X.; Sun, J.Q. Turning-lane and signal optimization at intersections with multiple objectives. *Eng. Optim.* **2019**, *51*, 484–502. [CrossRef]

34. Wong, C.K.; Heydecker, B.G. Optimal allocation of turns to lanes at an isolated signal-controlled junction. *Transp. Res. Part Methodol.* **2011**, *45*, 667–681. [CrossRef]

35. Lam, W.H.K.; Poon, A.C.K.; Mung, G.K.S. Integrated Model For Lane-Use And Signal-Phase Designs. *J. Transp. Eng.* **1997**, *123*, 114–122. [CrossRef]

36. Saneinejad, S.; Lo, J. Leading pedestrian interval: Assessment and implementation guidelines. *Transp. Res. Rec.* **2015**, *2519*, 85–94. [CrossRef]

37. Cubic Delivers on Productivity with the Next Generation of Enhancements to Synchro. Cubic Corporation. 2019. Available online: https://www.businesswire.com/news/home/20191119005371/en/Cubic-Delivers-on-Productivity-with-the-Next-Generation-of-Enhancements-to-Synchro (accessed on 26 September 2022).

38. Occupancy Rates of Passenger Vehicles. European Environment Agency. 2010. Available online: https://www.eea.europa.eu/data-and-maps/indicators/occupancy-rates-of-passenger-vehicles/occupancy-rates-of-passenger-vehicles (accessed on 26 September 2022).

39. Vehicle Occupancy Rates. In *Technical Report*; Office of Energy Efficiency & Renewable Energy: Washington, DC, USA, 2010.

40. Roshandeh, A.M.; Levinson, H.S.; Li, Z.; Patel, H.; Zhou, B. New methodology for intersection signal timing optimization to simultaneously minimize vehicle and pedestrian delays. *J. Transp. Eng.* **2014**, *140*, 4014009. [CrossRef]